Journal of Medicinal Chemistry

Article

Novel aryloxyethyl derivatives of 1-(1-benzoylpiperidin-4-yl)methanamine as the Extracellular Regulated Kinases 1/2 (ERK1/2) phosphorylation-preferring serotonin 5 HT1A receptor biased agonists with robust antidepressant-like activity

Joanna Sniecikowska, Monika G#uch-Lutwin, Adam Bucki, Anna Wi#ckowska, Agata Siwek, Magdalena Jastrz#bska-Wi#sek, Anna Partyka, Daria Wilczy#ska, Karolina Pytka, Krzysztof Pociecha, Agnieszka Cios, El#bieta Wyska, Anna Weso#owska, Maciej H. Paw#owski, Mark Varney, Adrian Newman-Tancredi, and Marcin Ko#aczkowski

J. Med. Chem., **Just Accepted Manuscript** • Publication Date (Web): 05 Feb 2019

Just Accepted

ACS Publications

is published by the American Chemical Society. 1155 Sixteenth Street N.W., Washington, DC 20036

Novel Aryloxyethyl Derivatives of 1-(1-benzoylpiperidin-4-yl)methanamine as the Extracellular Regulated Kinases 1/2 (ERK1/2) Phosphorylation-preferring Serotonin 5-HT_{1A} Receptor Biased Agonists with Robust Antidepressant-like Activity

*Joanna Sniecikowska [a], Monika Gluch-Lutwin [a], Adam Bucki [a], Anna Więckowska [a], Agata Siwek [a], Magdalena Jastrzebska-Wiesek [a], Anna Partyka [a], Daria Wilczyńska [a], Karolina Pytka [a], Krzysztof Pociecha [a], Agnieszka Cios [a], Elżbieta Wyska [a], Anna Wesołowska [a], Maciej Pawłowski [a], Mark Varney [b], Adrian Newman-Tancredi [b], Marcin Kolaczkowski [a]**

[a] Faculty of Pharmacy, Jagiellonian University Medical College, 9 Medyczna St., 30-688 Kraków, Poland;

[b] Neurolixis Inc. 34145 Pacific Coast Highway #504, Dana Point, CA 92629 USA

ABSTRACT

Novel 1-(1-benzoylpiperidin-4-yl)methanamine derivatives were designed as 'biased agonists' of serotonin 5-HT_{1A} receptors. Compounds were tested in signal transduction assays (ERK1/2 phosphorylation, cAMP inhibition, Ca^{2+} mobilization and β-arrestin recruitment) which identified ERK1/2 phosphorylation-preferring aryloxyethyl derivatives. The novel series showed high 5-HT_{1A} receptor affinity, >1000-fold selectivity versus noradrenergic α_1, dopamine D_2, 5-HT_{2A}, histamine H_1 and muscarinic M_1 receptors, and favorable drug-likeness properties (CNS-MPO, Fsp^3, LELP). The lead structure, (3-chloro-4-fluorophenyl)(4-fluoro-4-(((2-(pyridin-2-yloxy)ethyl)amino)methyl)piperidin-1-yl)methanone (**17,** NLX-204), displayed high selectivity in

the SafetyScreen44™ panel (including hERG channel), high solubility, metabolic stability and Caco-2 penetration, and did not block CYP3A4, CYP2D6 isoenzymes or P-glycoprotein. Preliminary *in vivo* studies confirmed its promising pharmacokinetic profile. **17** also robustly stimulated ERK1/2 phosphorylation in rat cortex and showed highly potent (MED=0.16 mg/kg) and efficacious antidepressant-like activity, totally eliminating immobility in the rat Porsolt test. These data suggest that the present 5-HT_{1A} receptor biased agonists could constitute promising antidepressant drug candidates.

INTRODUCTION

Despite the clinical availability of a large number of antidepressant drugs, the treatment of depressive disorders still remains an area of unmet medical need. With few exceptions, current antidepressants target inhibition of monoamine neurotransmitter reuptake into brain neurons.[1] The clinical efficacy of this strategy is less than optimal, as indicated by the substantial proportion of patients that fail to respond to treatment or that show only partial treatment response.[2,3] Furthermore, current antidepressants usually require several weeks of administration before clinical efficacy is observed – this protracted delay in therapeutic onset is a source of distress to families, of increased medical burden and of potential suicide risk for patients.[4,5] Nevertheless, recent findings suggest that the development of rapidly-acting and highly clinically-efficacious novel antidepressants is a realistic prospect. Indeed, the discovery that ketamine, a general anesthetic drug acting primarily as a non-competitive N-methyl-D-aspartate (NMDA) receptor antagonist, can reverse depressive symptoms in profoundly-depressed and treatment-resistant patients, has given new hope that depressive states can be treated efficaciously and rapidly. Accordingly, the S-enantiomer of ketamine is currently being evaluated by the FDA as a rapid-acting antidepressant for treatment-resistant depression.[6–8] At a molecular level, ketamine was found to mediate its antidepressant effects in rats via several mechanisms including AMPA and mTOR activation and, of particular interest in the present context, Extracellular Regulated Kinase (ERK) phosphorylation in prefrontal cortex. The latter mechanism has attracted considerable attention as a substrate for ketamine's antidepressant activity. Indeed, ketamine elicits robust phosphorylation of ERK in this brain region [9–11] and, correspondingly, inhibition of ERK phosphorylation using inhibitors of mitogen-activated proteins kinase (MEK) blocked the antidepressant-like effects of ketamine in rat models, an observation that was also seen with another NMDA receptor antagonist, Ro 25-6981.[12] These results strongly suggest that mechanisms

that elicit robust activation of cortical ERK phosphorylation could constitute an effective and novel strategy to discover improved antidepressant drugs which, like ketamine, could (i) show efficacy in profoundly-depressed and treatment-resistant patients, (ii) be effective following short durations of treatment (or even acutely, like ketamine), and (iii) target new neurobiological mechanisms distinct from classical monoamine reuptake inhibitors. Nevertheless, ketamine presents several notable limitations that prevent its widespread use as an antidepressant, including the induction of dissociative states which may be difficult to separate from the antidepressant effects,[13,14] cardiovascular and urinary tract side-effects,[15–17] as well as neurotoxicity and neurocognitive dysfunction. These considerations highlight the ongoing medical need for novel and well-tolerated antidepressant drugs. In the search for a suitable target to achieve such a profile, it is interesting that ketamine's mechanism of action involves serotonergic pathways and, notably, activation of the 5-HT_{1A} receptor subtype, at least in certain animal tests.[18–20] Presynaptic 5-HT_{1A} autoreceptors have been implicated in the delay of therapeutic onset of antidepressants but post-synaptic 5-HT_{1A} receptors, notably in cortical brain regions, are known to mediate potent antidepressant-like effects in animal models.[21–25] In addition, a moderately-selective 5-HT_{1A} receptor agonist, flesinoxan, was shown to have promising antidepressant properties,[26] whereas partial agonists at 5-HT_{1A} receptors (e.g. buspirone) have failed to show robust antidepressant effects. It therefore appears that full-agonist targeting of 5-HT_{1A} receptors may be a promising strategy for identification of novel antidepressants, potentially mimicking the remarkable antidepressant effects of ketamine. However, targeting of 5-HT_{1A} receptors may require preferential activation in specific brain regions, notably frontal cortex. Although there is only a single gene sequence for 5-HT_{1A} receptors, which does not contain introns or splice variants, the effects of 5-HT_{1A} receptor activation in different brain regions can be quite diverse, and even divergent, due to coupling of the receptors

to distinct signal transduction responses. Thus, although the amino acid sequence of the 5-HT_{1A} receptor itself is unchanged, the latter's interaction with intracellular signaling proteins varies depending on brain region. Thus, if agonists preferentially elicit coupling of the receptors to particular G-proteins or second messengers, this would be anticipated to results in preferential activation of distinct brain regions.

The recent discovery and characterization of 5-HT_{1A} receptor biased agonists offer a way forward in this respect. F15599 (**1**), also known as NLX-101, is a highly-selective 5-HT_{1A} receptor agonist with a unique profile, preferentially activating ERK phosphorylation versus other signaling pathways *in vitro*,[27] as well as *ex vivo* in frontal cortex.[28] Notably, **1** elicited strong antidepressant-like activity in the rat forced swim test, completely abolishing immobility, even upon acute administration – as is the case with ketamine, suggesting that the preferential activation of cortical ERK phosphorylation via cortical 5-HT_{1A} receptors translates to enhanced antidepressant potential.[29–31]

However, **1** has so far been the only compound displaying such a promising 'biased agonist' profile of activity, and some close chemical analogues (notably F13714 or befiradol) display quite different signal transduction properties *in vitro* and *in vivo*.[31–35] In addition, the latter compounds do not exhibit preferential activation of cortical 5-HT_{1A} receptors which, as discussed above, is important for improved antidepressant activity.[29,36,37] The structure-activity relationships of these compounds with respect to preferential ERK phosphorylation have not been established and it therefore remains to be determined whether increased 'bias' for ERK phosphorylation can elicit even superior antidepressant profiles.

Based on these considerations, the present work used **1** as a model structure to explore the synthesis and characterization of a series of novel 5-HT_{1A} receptor-targeted antidepressants. In order to establish their comprehensive functional selectivity profiles, the whole novel series was tested in four signal transduction assays (ERK1/2 phosphorylation, cAMP inhibition, Ca^{2+} mobilization and β-arrestin recruitment), for the first time in the case of the 5-HT_{1A} receptor agonists. Specifically, we sought to identify the structural motifs that confer a 'biased' ERK-preferential activity of the compounds as well as to determine whether they possess favorable drug-like properties that are compatible with successful pharmaceutical development. Finally, to confirm the therapeutic potential of the series, we tested a lead compound in a recognized *in vivo* model of antidepressant-like activity.

RESULTS AND DISCUSSION

Design, synthesis and biological evaluation of 1-(1-benzoylpiperidin-4-yl)methanamine derivatives

As a framework for the design of novel compounds we used docking-derived ligand-receptor complex of **1** in the homology model of the 5-HT_{1A} receptor[38] (Figure 1). The analysis of the binding mode revealed crucial interactions, commonly found for a vast majority of monoaminergic ligands, namely (*i*) charge-reinforced hydrogen bond between the protonated central nitrogen atom and the carboxyl group of the aspartic acid Asp3.32 as well as (*ii*) CH–π stacking between the pyrimidine ring and phenylalanine Phe6.52. The additional interactions included (*iii*) a hydrogen bond between the oxygen atom of the amide moiety and the NH group from the main chain of the isoleucine Ile189 in the second extracellular loop, (*iv*) π–π stacking between the benzoyl moiety and phenylalanine Phe3.28 as well as (*v*) cation–π interaction between the protonated central nitrogen atom and phenylalanine Phe6.51.

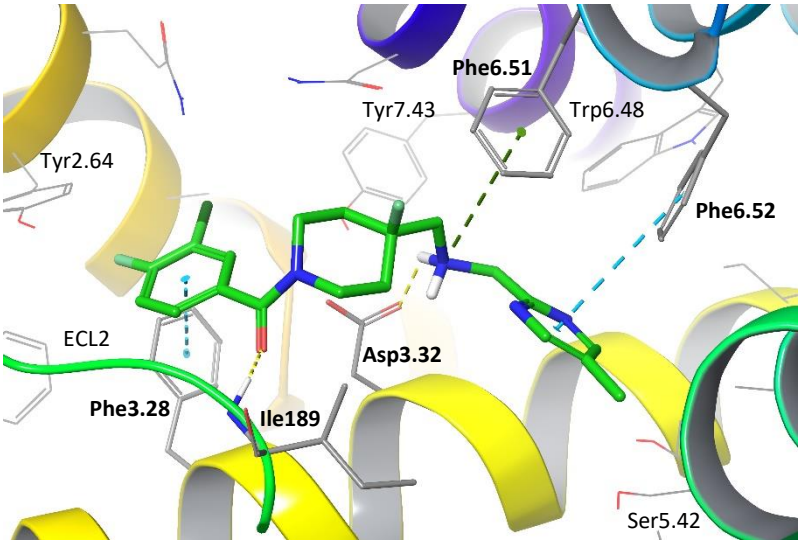

Figure 1. The predicted binding mode of compound **1** in the site of serotonin 5-HT_{1A} receptor. Amino acid residues engaged in ligand binding (within 4Å from the ligand atoms) are displayed as sticks, whereas crucial residues, e.g. forming H-bonds (dotted yellow lines), π-π/CH-π stacking (dotted cyan lines) and cation-π interactions (dotted green

line) are represented as thick sticks. ECL2 residues were hidden for clarity; ECL – extracellular loop. The homology model of the 5-HT_{1A} receptor prepared based on crystal structure of the 5-HT_{1B} receptor (PDB ID: 4IAR).

Although the observed interactions seem to be optimal for binding to the 5-HT_{1A} receptor, we have noticed that the pyrimidine ring does not fully penetrate the hydrophobic binding pocket of the receptor. At this point it is worth noting that this region of the binding site of GPCRs accommodates moieties that are crucial for eliciting particular functional activity.[39] Thus, we hypothesized that diversification of the fragment of the molecule that binds within the pocket may yield compounds with various functional profiles. In our attempt to develop novel ligands that would more effectively fill this hydrophobic binding pocket, we initially focused on extension of the one-unit methylene linker to three-unit linker between the central amine function and pyrimidine ring of **1**. We introduced a propylene linker and a number of analogues with one of the methylene units replaced with heteroatoms such as nitrogen, sulfur and oxygen (Figure 2).

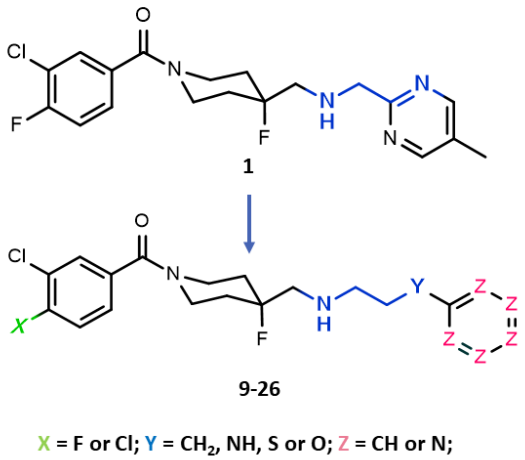

Figure 2. General structure of the new series of selective 5-HT_{1A} receptor agonists.

We have validated our hypothesis in the docking studies where we compared the binding modes of **1** and newly designed ligands, exemplified by compounds **16** and **17** (Figure 3). As expected, the extension of the linker shifted the aromatic ring towards Phe6.52, markedly shortening the CH-

π bond (3.27 Å for **1** vs. 2.85 Å and 2.96 Å for compounds **16** and **17**, respectively) and optimizing the geometry of the interactions. The derivatives with three-unit linkers more effectively filled the hydrophobic binding pocket near the transmembrane helix 6 (TMH6), which accounted for better fitting to the receptor and promoted the reduction of binding energy. Encouraged by the results of docking studies, we moved to the synthesis and biological evaluation of the compounds.

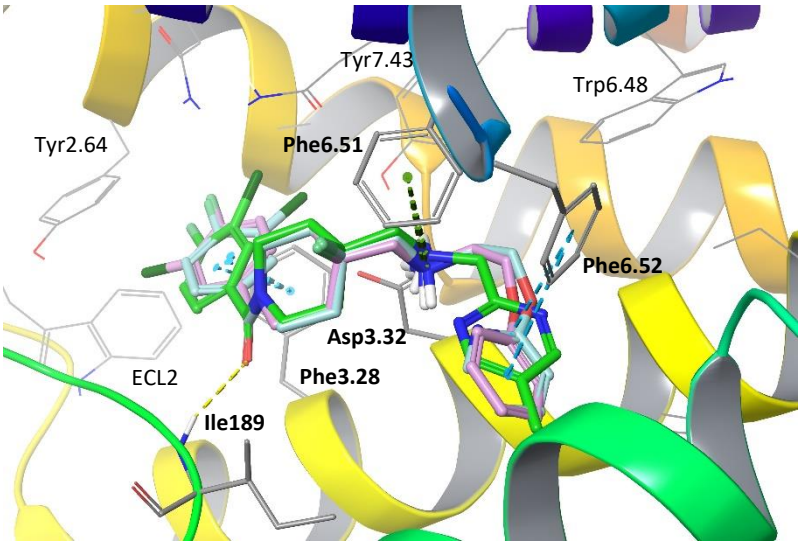

Figure 3. The predicted binding mode of compound **1** (green) together with **16** (pink) and **17** (white) in the site of the serotonin 5-HT_{1A} receptor. Amino acid residues engaged in ligand binding (within 4Å from the ligand atoms) are displayed as sticks, whereas crucial residues, e.g. forming H-bonds (dotted yellow lines), π-π/CH-π stacking (dotted cyan lines) and cation-π interactions (dotted green line) are represented as thick sticks. ECL2 residues were hidden for clarity; ECL – extracellular loop. The homology model of the 5-HT_{1A} receptor prepared based on crystal structure of the 5-HT_{1B} receptor (PDB ID: 4IAR).

The synthetic pathway to the target compounds was based on the one previously developed and reported, [40,41] as presented in Scheme 1.

Scheme 1. Synthesis of 1-(1-benzoyl-4-fluoropiperidin-4-yl)methanamine derivatives[a]

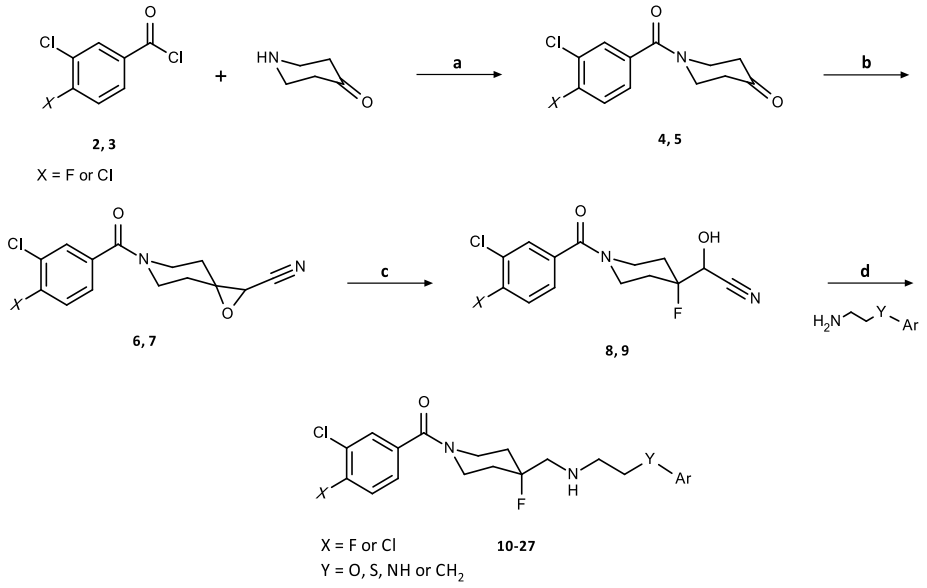

[a] Reagents and conditions: (a) Et_3N, DCM, 0 °C then r.t., 12 h, yield: 47–60%; (b) chloroacetonitrile, 30% NaOH, TBABr, DCM, r.t., 3 h, yield: 80–87%; (c) HF/pyridine, DCM, -10 °C, 30 min then r.t. 24–36 h, yield: 54–68%; (d) DABCO, $NaCNBH_3$, $FeSO_4 \times 7H_2O$, molecular sieves, MeOH, r.t., 36–72 h, yield: 23–66%.

In the first step, the commercially available 4-piperidone was acylated by the appropriate benzoyl chloride derivatives **2** or **3** in the presence of triethylamine. Then a Darzens reaction between the obtained benzoylpiperidin-4-one derivatives **4** or **5** and chloroacetonitrile, using tetrabutylammonium bromide as a phase transfer catalyst,[42] gave the corresponding cyanoepoxides **6** or **7**. The epoxides **6** or **7** underwent a regioselective ring opening reaction with poly(hydrogen fluoride)pyridine[43,44] to obtain the corresponding cyanohydrins **8** or **9**. The final compounds **9–27** were prepared via reductive amination using cyanohydrins **8** or **9** and the appropriate amines in the presence of a base and sodium cyanoborohydride as reducing agent and with addition of iron sulfate heptahydrate.[41]

The affinity of the compounds for the 5-HT_{1A} receptor was determined in radioligand binding assay (Table 1). All but one (compound **11**) displayed affinities higher than that of **1**, with pK_i values ranging from 8.73 to 10.83 vs 8.66 for **1**. The affinity was most significantly increased for the compounds with oxyethylene linker (**16–19**), which showed subnanomolar affinities (pK_i = 10.19–10.83). These results unequivocally confirmed our hypothesis derived from molecular modeling and allowed us to choose oxyethylene linker for further studies. The superiority of the oxyethylene linker over other linkers tested may be due to the fact that oxygen atom is the best bioisostere of the crucial nitrogen atom embedded in the aromatic moiety of **1** (electronegative, H-bond accepting). At this stage we tested *para* position of the benzoyl fragment, by the replacement of fluorine with chlorine atom (compounds **18** and **19**). This modification increased binding affinity (**18** vs **16** and **19** vs **17**), but comparison of LELP scores showed that it had resulted from increase in lipophilicity and most probably non-specific interactions. Therefore, we used 3-chloro-4-fluorobenzoil core in further studies.

Table 1. 5-HT$_{1A}$ receptor affinity and developability parameters of compounds **10**–**19** and the references.

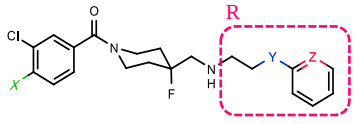

Compd	X	R	receptor affinity[a] (pK_i) 5-HT$_{1A}$[b,d]	α_1[c,e]	D_2[b,f]	Fsp^3[g]	LELP[h]	CNS MPO[i]
10	F	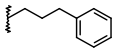	9.32 ± 0.19	< 6.00	< 6.00	0.41	9.1	4.06
11	F	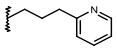	8.59 ± 0.01	6.75 ± 0.02	< 6.00	0.43	6.8	5.11
12	F	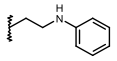	8.73 ± 0.06	< 6.00	< 6.00	0.38	7.0	4.93
13	F	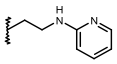	8.90 ± 0.15	7.26 ± 0.07	< 6.00	0.40	5.5	5.08
14	F	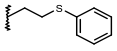	9.25 ± 0.21	NT[j]	< 6.00	0.38	8.6	3.86
15	F	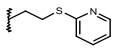	9.21 ± 0.04	7.63 ± 0.18	< 6.00	0.40	7.2	4.86
16	F	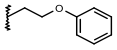	10.21 ± 0.20	6.29 ± 0.13	< 6.00	0.38	6.7	4.89
17	F	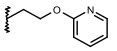	10.19 ± 0.19	6.78 ± 0.05	< 6.00	0.40	5.5	5.42
18	Cl	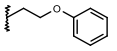	10.83 ± 0.15	NT	< 6.00	0.38	7.2	4.31
19	Cl	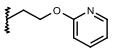	10.47 ± 0.20	6.89 ± 0.00	< 6.00	0.40	6.2	4.93
1			8.66 ± 0.07	< 6.00	< 6.00	0.42	5.2	5.44
8-OH-DPAT			9.09 ± 0.03	NT	NT	0.62	5.9	3.41
Buspirone			8.30 ± 0.05	NT	NT	0.71	4.3	5.82

[a] All binding affinity values are represented as pK_i i.e. –logK_i and expressed as means ± SEM from at least 3 experiments performed in duplicates; Radioligand binding was performed using [b] CHO-K1 cells, [c] rat cortex; The affinity values were determined using [d] [^{3}H]8-OH-DPAT, [e] [^{3}H]-prazosin, phentolamine pKi = 7.95, [f] [^{3}H]-methylspiperone, haloperidol pK_i = 8.85; [g] fraction of sp^3 carbon atoms; [h] ligand efficiency-dependent lipophilicity score; [i] Central Nervous System Multiparameter Optimization score; [j] NT – not tested.

Next, we explored the optimal position of a nitrogen atom in the aryloxy moiety (Table 2). We observed a gradual decrease in binding affinity to a pK_i of 8.82 for pyridin-3-yloxy derivative (**20**) and an unacceptably low binding value (pK_i 6.41) for pyridin-4-yloxy derivative (**21**).

Table 2. 5-HT$_{1A}$ receptor affinity and developability parameters of compound's **17** analogs **20**–**27**.

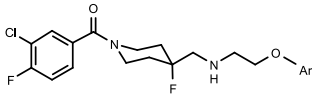

		receptor affinity[a] (pK_i)					
Compd	**Ar**	**5-HT$_{1A}$**[b,d]	**α_1**[c,e]	**D$_2$**[b,f]	**Fsp^3**[g]	**LELP**[h]	**CNS MPO**[i]
17		10.19 ± 0.19	6.78 ± 0.05	< 6.00	0.40	5.5	5.42
20		8.82 ± 0.06	< 6.00	< 6.00	0.40	5.0	5.65
21		6.41 ± 0.13	< 6.00	< 6.00	0.40	6.9	5.41
22		9.28 ± 0.10	< 6.00	< 6.00	0.42	3.4	5.46
23		7.45 ± 0.10	< 6.00	< 6.00	0.42	5.9	5.47
24		6.68 ± 0.16	< 6.00	< 6.00	0.42	4.5	5.44
25		6.70 ± 0.12	< 6.00	< 6.00	0.42	3.7	5.44
26		8.42 ± 0.20	< 6.00	< 6.00	0.43	8.2	4.90
27		7.86 ± 0.13	< 6.00	< 6.00	0.45	7.1	5.37

[a] All the binding affinity values were represented as pK_i i.e. –logK_i and expressed as means ± SEM from at least 3 experiments performed in duplicates; Radioligand binding was performed using [b] CHO-K1 cells, [c] rat cortex; The affinity values were determined using [d] [^{3}H]8-OH-DPAT, [e] [^{3}H]-prazosin, phentolamine pK_i = 7.95, [f] [^{3}H]-methylspiperone , haloperidol pK_i = 8.85; [g] fraction of sp^3 carbon atoms; [h] ligand efficiency-dependent lipophilicity score; [i] Central Nervous System Multiparameter Optimization score;

Subsequently, we explored heterocycles with two nitrogen atoms (**22**–**25**). Only 2-pyrazine derivative, compound **22** with pK_i 9.28 kept the desired level of affinity (pK_i >8). Interestingly, **22** can be considered a hybrid of 2- and 3-pyridine and its pK_i value is intermediate between that of **17** (10.19) and that of **20** (8.82). We have also prepared compound **26** that is a direct analog of befiradol and compound **27** – an analogue of **1** to invesitgate the effect of methyl substituent at the 5 position of the aryl ring. Compound **26** displayed significantly decreased affinity compared to compound **17** (pK_i 8.42 vs. 10.19, respectively) while compound **27** showed a modest increase in

affinity relative to its unsubstituted analog **23** (pK_i 7.86 vs. 7.45, respectively). These contrasting results indicate that the substitution pattern at the aromatic ring will require further investigation.

Developability analysis – *In silico*-supported predictions

In order to provide an early assessment of the developability of the designed series, we analyzed all the compounds using *in silico*-supported measures of drug-likeness. All the compounds fulfilled Lipinski's rule of five (Ro5) for good oral bioavailability and displayed exceptionally high Central Nervous System Multiparameter Optimization (CNS MPO) values with median value of 5.10. [45,46]

Another important parameter that is especially important in the context of compounds' solubility is the fraction of sp^3 atoms (Fsp^3). A majority of the compounds tested, mostly those with two nitrogen atoms in the aryl ring, showed very high and favorable Fsp^3 values of 0.42–0.45, while all the others were characterized by acceptable values of 0.38–0.41. [47]

Next, we used ligand efficiency dependent lipophilicity (LELP), a function that combines physicochemical properties with compounds' activity to predict druglikeness. The median LELP value for all the compounds was 6.75, which is the desirable value for drug candidates.[48,49] Six compounds displayed excellent values $\leq$ 5.9, reaching an exceptionally favorable value for compound **22** (LELP = 3.4) (Tables 1 and 2).

Finally, we have used SwissADME web tool [50–53] to identify Pan-Assay INterference compoundS (PAINS) as well as toxicophores within the investigated group of compounds. The analysis showed no alerts for any of the tested compounds.

Summing up, the vast majority of the designed compounds were characterized by favorable values of physicochemical properties and multivariate scoring functions, as well as good results of safety filters, which suggest a favorable developability potential of the designed series.

Developability analysis – *In vitro* assays

Next, to confirm the favorable developability profile predicted *in silico*, compound **17** was selected as a lead structure, to be examined in a series of *in vitro* experiments. To this end, the SafetyScreen44™ Panel (plus additional antitargets), the Bioavailability Panel, as well as CYP3A4, CYP2D6 and P-glycoprotein (P-gp) inhibition assays, were performed at Eurofins Pharma Discovery Services. SafetyScreen44™ Panel is one of the most commonly used set of assays for *in vitro* pharmacological profiling of target selectivity. [54] Bioavailability Panel consists of solubility, permeability, protein binding and metabolic stability assays, which are used for prediction of ADME properties, a very important issue in the drug development process.

Data from the safety pharmacology profiling revealed excellent overall selectivity of the investigated lead structure. Compound **17**, tested at a concentration of 10 μM, showed substantial binding inhibition (higher than 50%) for only 3 among 52 off-targets, namely: adrenergic α_{1A} and α_{2A} and dopaminergic D_{2S} receptors (91–99%) (Table 3). Compound **17** was subsequently tested at a concentration of 1 μM for these antitargets and exhibited much lower binding inhibition at D_2 (9.5%) and α_{2A} (29.9%) receptors but maintained a relatively high value for α_{1A} receptor (87.6%). The precise affinity for the latter was therefore determined and the pK_i was found to be 6.78, an affinity which is more than 1000-fold lower than the affinity of compound **17** for the 5-HT_{1A} receptor (pK_i = 10.19; see Table 1). In addition to testing the binding affinity of **17** for hERG channel in the SafetyScreen44^{TM}, we also tested it using an automated patch-clamp method. Patch

clamp methods are considered to provide a more reliable assessment of hERG interaction, even at an early stage of drug discovery process.[55,56,57] This study was performed at 3 concentrations (10.0, 1.0 and 0.1 μM) showing only 0.1, 10.5 and 46.5% inhibition of tail current respectively. This indicates that **17** has a low propensity for hERG channel blockade and suggests that the investigated series has a low risk with respect to hERG-related cardiac safety.

In the Bioavailability Panel, compound **17** exhibited desirable druglike ADME attributes (Table 4). It was characterized by high aqueous solubility in phosphate-buffered saline (PBS 7.4), simulated intestinal fluid (SIF) and simulated gastric fluid (SGF) (192.2, 192.2 and 200 μM, respectively) as well as excellent permeability on Caco-2 cells (Papp > 10×10^{-6} cm/s). Moreover, final efflux ratio value (ER = basolateral to apical [BA]/apical to basolateral [AB] permeability) was lower than 2.5 (ER = 0.86), which means that compound **17** is not a P-gp substrate.[46] Those values are comparable with the reference drug propranolol, which belongs to the class 1 of Biopharmaceutics Classification System (BCS) – high permeability/high solubility – suggesting good oral absorption and reliable *in vitro-in vivo* correlation.[58]

Table 3. SafetyScreen44™ Panel and additional antitargets results for compound **17**.

Target	Assay	% inhibition of Control Specific Binding at 10 µM/1 µM[a]	Target	Assay	% inhibition of Control Specific Binding at 10 µM/1 µM[a]
GPCR			**GPCR**		
ADENOSINE	**A_{2A}**	11.8	SEROTONIN	**5-HT_{1B}**	-9.1
ADRENERGIC	**α_{1A}**	99.7/87.6		**5-HT_{1D}**	NT/25.5
	α_{1B}	NT/32.2		**5-HT_{2A}**	9.0
	α_{2A}	94.3/29.9		**5-HT_{2B}**	39.7
	β_1	2.2		**5-HT_{2C}**	NT/-26.2
	β_2	3.8		**5-HT_6**	NT/12.1
CANNABINOID	**CB_1**	0.4		**5-HT_7**	NT/13.2
	CB_2	-3.1*	**TRANSPORTERS**		
CHOLECYSTOKININ	**CCK_1 (CCK_A)**	-30.3	DOPAMINE	**DAT**	20.4
DOPAMINE	**D_1**	38.2	NOREPINEPHRINE	**NET**	-2.0
	D_{2S}	91.3/9.5	SEROTONIN	**SERT**	0.9
	D_3	NT/39.1	**ION CHANNELS**		
ENDOTHELIN	**ET_A**	-13.8	GABA CHANNEL	**BZD** (central)	-11.8
HISTAMINE	**H_1**	-0.5	GLUTAMATE CHANNEL	**NMDA**	-1.8
	H_2	-15.1	NICOTINIC CHANNEL	**N** neuronal **α4β2**	-5.4
	H_3	NT/-10.9	SEROTONIN CHANNEL	**5-HT_3**	-12.7
	H_4	NT/-10.9	Ca^{2+} CHANNEL	**Ca2+ channel (L)** (dihydropyridine site)	18.2
MUSCARINIC	**M_1**	12.9	K^+ CHANNELS	**hERG** ([^{3}H]Dofetilide)	16.2
	M_2	6.3		**K_v channel**	3.8
	M_3	9.7	Na^+ CHANNEL	**Na^+ channel** (site 2)	48.8
	M_4	NT/8.8	**KINASES**		
OPIOID & OPIOID LIKE	**δ_2 (DOP)**	7.2	CTK	**Lck kinase**	18.2
	κ (KOP)	34.6	**OTHER NON-KINASE ENZYMES**		
	µ (MOP)	42.9	AA METABOLISM	**COX_1**	11.9
VASOPRESIN	**V_{1a}**	7.0		**COX_2**	-9.2
			MONOAMINE & NEUROTRANSMITTER	**AChE**	-2.9
NUCLEAR RECEPTORS				**MAO-A**	-3.6
STEROID NUCLEAR RECEPTORS	**AR**	-20.5	PHOSPHODIESTERASES	**PDE3A**	-3.9
	GR	-5.1		**PDE4D2**	-10.7

[a] Assays, in which % inhibition of Control Specific Binding was over 50% in 10 µM, were repeated at 1 µM concentration. For some targets only the test at 1 µM was performed – marked as NT/value. *Low to moderate negative values (< 50%) have no real meaning and are attributable to variability of the signal around the control level;

Compound **17** also exhibited high microsomal stability, with intrinsic clearance (CL_{int}) lower than 115 [μL/min/mg] and a half-life higher than 60 minutes. Noteworthy, it is the best possible result in the given experimental setting, suggesting high metabolic stability and therefore a low risk of significant first pass effect. Overall, the above-mentioned results suggest favorable oral bioavailability of compound **17** and are in line with the favorable CNS MPO (5.42), Fsp^3 (0.40) and LELP (5.5) values predicted *in silico* for compound **17**. Furthermore, compound **17** displayed no P-gp inhibition (6.5% of inhibition at 10 μM) as well as negligible inhibition of CYP3A4 and CYP2D6 (23.2% and 15.9% at 10 μM, respectively). Together with the moderate plasma protein binding (93.2%), this suggests a relatively low drug–drug interaction potential. Taken together, these data provide compelling evidence supporting desirable druglike properties of compound **17**, suggesting its good developability potential and promising similarly favorable properties for the whole series.

Table 4. *In vitro* Bioavailability Panel and CYP3A4, CYP2D6 and P-gp inhibition assays results for compound **17.**

Assay		Compound 17 (10 μM*)	Reference
Solubility [45]	PBS[a]	192.2 μM	180.8 μM (metoprolol)
	SGF[b]	200 μM	–
	SIF[c]	192.2 μM	–
Permeability [59]	A–B[d]	25.90 [10^{-6} cm/s]	23.70 [10^{-6} cm/s] (propranolol)
	B–A[d]	22.45 [10^{-6} cm/s]	27.40 [10^{-6} cm/s] (propranolol)
Metabolic stability[e] [60]	Intrinsic Clearance (CL_{int})	< 115 [μL/min/mg]	< 115 [μL/min/mg] (propranolol)
	Half-Life ($T_{1/2}$)	> 60 [min]	> 60 [min] (propranolol)
Protein binding[f] [61]		93.2%	99% (warfarin)
P-gp inhibition[g] [62]		6.5%	15 μM [IC_{50}] (verapamil)
CYP3A4 inhibition[h] [63]		23.2%	0.24 μM [IC_{50}] (ketoconazole)
CYP2D6 inhibition[h] [64]		15.9%	0.0081 μM [IC_{50}] (quinidine)

*Metabolic stability study was performed at the concentration of 0.1 μM; Solubility study was performed in a 200 μM concentration; [a] aqueous solubility at buffer pH7.4; [b] aqueous solubility in simulated gastric fluid; [c] aqueous solubility at simulated intestinal fluid; [d] Caco-2, pH 6.5/7.4; [e] liver microsomes–human; [f] plasma human; [g] MDR1-MDCKII cell line; [h] Human recombinant

Selectivity vs. key antitargets

As the goal of the present study was to obtain selective 5-HT_{1A} receptor agonists, it was essential to verify the selectivity of the novel ligands. To this end, the affinity for the most important antitargets was determined for all of the obtained compounds. The determination of the affinities for α_1 and D_2 receptors was prioritized because activities at such receptors may interfere *in vivo* with the activity elicited by 5-HT_{1A} receptor activation.[65–67] Moreover, the pertinence of testing those targets was also highlighted by the results of SafetyScreen44 for compound **17**, which showed relatively higher affinity for α_1 and D_2 receptors than for other off-targets. Concerning α_1 receptor affinity, the majority of the compounds showed substantial selectivity for 5-HT_{1A} receptor (over 1000–10000-fold). Selectivity dropped lower than 100-fold only for compounds **11**, **13** and **15**, which are pyridine analogs with non-oxygen linker. In the case of the D_2 receptor, none of the

compounds had pK_i over 6 (Tables 1 and 2). Additionally, we examined the binding affinity of each compound for serotonin 5-HT_{2A}, muscarinic M_1 and histamine H_1 receptors (see Supporting Information Table S3). None of the tested compounds exceed 50% of control specific binding at a concentration of 1 μM in these assays.

Considering the above and bearing in mind that the selected lead structure **17** showed substantial selectivity also vs. the other 49 off-targets (Table 3), it may be concluded that the designed series is characterized by a high selectivity for 5-HT_{1A} receptors.

Structure-Functional Activity Relationships

To investigate the functional profiles of the presented series we evaluated functional activity of twelve selected compounds (**10**–**17**, **19**, **20**, **22** and **27**) in the following pathways engaged in 5-HT_{1A} receptor signal transduction: ERK1/2 phosphorylation (pERK1/2), adenylyl cyclase inhibition (cAMP), β-arrestin recruitment (β-arrestin) and calcium mobilization (Ca^{2+}) (Figure 4).

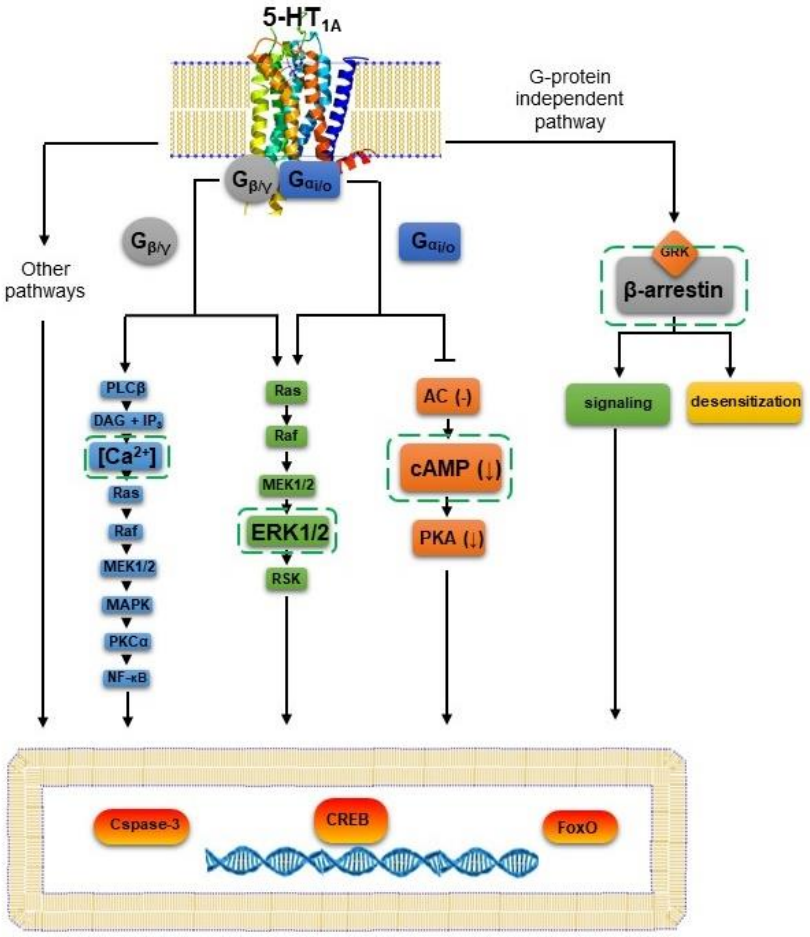

Figure 4. Signaling pathways measured after activation of 5-HT_{1A} receptor; adopted from Chilmonczyk et. al. [68] and modified based on Rojas & Fiedler.[69]

To our knowledge, the present study is the first in which such a large number of 5-HT_{1A} receptor ligands was tested in such a number of intracellular signaling tests. This is also only the second study in which 5-HT_{1A} receptor ligands were examined for β-arrestin recruitment.[70] Here, we assumed that E_{max} values higher than 80% relative to the maximal effect of serotonin are characteristic of a full agonist, E_{max} values between 79% and 21% indicate a partial agonist and E_{max} values 20% or less are indicative of an antagonist. The experiments were carried out using cell lines expressing the recombinant human 5-HT_{1A} receptor. Although such cell lines may differ from neuronal systems e.g. as concerns their signal transduction machinery or receptor expression

levels (336 fmol/mg for CHO-K1 cells and 78 fmol/mg for U2OS cells), they provide an experimentally robust and widely accepted means of comparing drug activities and conducting SAR studies. In the case of the investigated series, the aryloxyethanamine derivatives (**16**, **17** and **19**) were the ones that showed the highest potency in functional activity assays (Table 5), as discussed in greater detail below. Dose-response curves for functional activity of all the compounds are presented in Supporting Information.

ERK1/2 phosphorylation

Derivatives containing S, NH or CH_2 in the linker were over one order of magnitude weaker than their aryloxyethanamine derivatives, with the compound **14** (phenylsulfanylethanamine derivative), exhibiting the lowest intrinsic activity in this pathway (pEC_{50} = 6.77). Except for compounds **14** and **15**, no potency differentiation between phenyl derivatives and their pyridine counterparts, as well as between 3-chloro-4-fluorobenzoyl derivative (**17**) and its 3,4-dichlorobenzoyl analog (**19**) were observed. The potencies of aryloxyethanamines were higher than those of all references, including **1**.

In contrast to buspirone, agonist efficacy (E_{max}) of all the tested compounds was high, i.e. between 77% and 95%. The highest agonist efficacy, comparable with 8-OH-DPAT, was observed for compounds **11** and **16**, however none of the compounds reached the 100% efficacy level of **1**.

Table 5. Functional activity of compounds **10**–**17**, **19** and references at 5-HT_{1A} receptors.

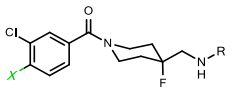

			5-HT_{1A} receptor functional activity[a]							
			ERK1/2[b]		cAMP[b]		β-arrestin[c]		Ca^{2+} [b]	
Compd	***X***	**R**	***E*MAX**	**pEC50**	***E*MAX**	**pEC50**	***E*MAX**	**pEC50**	***E*MAX**	**pEC50**
10	F	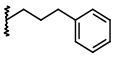	77%	**7.88**	91%	**7.10**	99%	**6.35**	74%	**7.07**
11	F	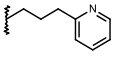	95%	**7.90**	74%	**7.33**	101%	**6.94**	87%	**7.84**
12	F	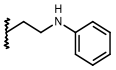	81%	**7.59**	79%	**6.73**	104%	**5.70**	65%	**6.98**
13	F	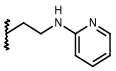	83%	**7.76**	86%	**7.26**	99%	**6.58**	52%	**7.13**
14	F	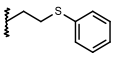	85%	**6.77**	71%	**5.61**	70%	**5.44**	NT	**NT**
15	F	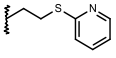	84%	**7.89**	76%	**7.18**	102%	**6.54**	73%	**6.95**
16	F	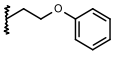	92%	**9.10**	90%	**8.09**	96%	**7.98**	52%	**7.39**
17	F	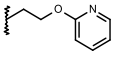	81%	**9.37**	89%	**8.05**	98%	**7.68**	57%	**7.76**
19	Cl	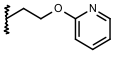	85%	**9.06**	71%	**8.04**	99%	**6.76**	58%	**7.41**
20	F	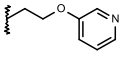	99%	**7.62**	100%	**7.32**	101%	**6.87**	98%	**7.34**
22	F	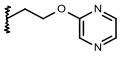	100%	**8.31**	90%	**7.68**	97%	**7.60**	89%	**7.54**
27	F	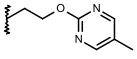	72%	**7.28**	41%	**6.03**	75%	**5.56**	NT[d]	**NT**
1			100%	**8.33**	92%	**7.22**	98%	**6.71**	60%	**6.61**
8-OH-DPAT			93%	**8.09**	63%	**7.50**	101%	**7.84**	NT	**NT**
Buspirone			44%	**7.82**	49%	**7.14**	100%	**6.73**	NT	**NT**
Serotonin			100%	**7.48**	100%	**7.51**	100%	**6.89**	100%	**7.30**

[a] All the functional activity values were expressed as means from at least 3 experiments performed in duplicates. For the sake of clarity, the SEM values were omitted in this table and presented in the supporting information – Table 3; The functional assay was performed using [b] CHO-K1 cells, [c] U2OS cells (Tango LiveBLAzer assay kit) ; [d] NT – not tested

Inhibition of cAMP production (cAMP)

Among the most potent derivatives with oxyethylene linker, no differences between the phenyl derivative and the pyridine analog were observed. By contrast, in the case of aminoethylene and sulfanylethylene linker, the pyridine counterparts showed higher cAMP potency than their phenyl derivatives (**15** and **13** vs. **14** and **12**). Potencies of the most active compounds (**16**, **17** and **19**) were higher than those of reference compounds.

In the case of agonist efficacy, most of the compounds behaved as partial agonists, however their efficacy was higher (71–79%) than for the reference partial agonists, buspirone and 8-OH-DPAT (49% and 63% respectively). Compounds **10**, **13**, **16**, and **17** were full agonists with efficacy (86–91%) comparable to **1**. There were no marked differences between the pyridine and phenyl derivatives, except for the analogs with propylene linker, where phenyl derivative **10** was a full agonist (91%) while its pyridine counterpart **11** behaved as a partial agonist (74%).

β-arrestin recruitment (β-arrestin)

In the case of the analogs with oxyethylene linker, the pyridine derivatives were weaker than their phenyl counterparts, whereas in the case of other linkers they had higher potency. Similarly to previously discussed pathways, 3,4-dichlorobenzoyl analog showed lower potency than its 3-chloro-4-fluoro- counterpart. In this pathway, the most active compounds showed potency comparable to that of 8-OH-DPAT, and higher than **1** and buspirone.

Only a phenylsulphanyl derivative **14** behaved as a partial agonist (70%). The other compounds exhibited E_{max} values close to 100%, similar to that seen for the reference compounds.

Calcium mobilization (Ca^{2+}).

In this assay, the pyridine derivatives showed higher potency than their phenyl analogues. All the tested compounds had pEC_{50} values higher than that of **1**, with the most potent being **11** and **17**.

In comparison to other pathways, efficacies in the calcium mobilization assay were markedly lower, with all compounds except **11** being partial agonists (52–74%). The propylene derivatives **10** and **11** displayed the highest efficacy (74% and 87% respectively).

Functional activity of the compound 17 analogs: 20, 22 and 27

Changing the position of nitrogen atom in the aryloxyl moiety from 2 to 3, as well as replacement of 2-pyridine by 2-pyrimidine and 2-pyrazine resulted in decreased potency in each of the pathways. Pyrazin-2-yloxy derivative **22** was the most potent compound in this group and exhibited potency in a range from 7.54 in calcium mobilisation assay to 8.31 in the ERK1/2 phosphorylation assay. Similarly to affinity results, the pEC_{50} values of compound **22** are intermediate between pEC_{50} values for pyridin-2-yloxy (**17**) and pyridin-3-yloxy (**20**) derivatives. The 5-methylpyrimidin-2-yloxy derivative **27** showed the lowest potency.Compounds **20** and **22** displayed high agonist efficacy (89–101%) in all the performed assays, showing higher efficacy levels than **17**, especially in the case of ERK1/2 phosphorylation and calcium mobilisation. By contrast, compound **27** behaved as a partial agonist in all the pathways (41–75%, with exception of calcium mobilisation, where it was not tested).

Bias factors

In order to determine functional selectivity of the tested ligands, bias factors between particular pathways were calculated, according to the following equation: [71–74]

$$\text{Bias factor} = \log\left(\frac{\text{relative activity}_{\mathbf{12},\text{lig}}}{\text{relative activity}_{\mathbf{12},\text{ref}}}\right) =$$

$$= \log\left(\left(\frac{E_{\max_{\text{path1}}} \times \text{EC}_{50-\text{path2}}}{\text{EC}_{50-\text{path1}} \times E_{\max_{\text{path2}}}}\right)_{\text{lig}} \div \left(\frac{E_{\max_{\text{path1}}} \times \text{EC}_{50-\text{path2}}}{\text{EC}_{50-\text{path1}} \times E_{\max_{\text{path2}}}}\right)_{\text{ref}}\right)$$

Bias factor ensures equal comparison between all the pathways, considering the differences in EC_{50} and E_{max} values of both a test ligand and a reference agonist, which was serotonin in this case. Results for all the compounds were presented in Table 6. Compounds which displayed bias factor higher than 1 (equaling to >10× preference) were highlighted in green (for positive values) and in blue (for negative values). Those compounds which showed significant bias, but with pEC_{50} values which were relatively low (<8 in all assays), were considered less interesting and marked in gray.

Table 6. Bias factors of compounds **10**–**17**, **19**, **20**, **22**, **27** and references at 5-HT_{1A} receptors.

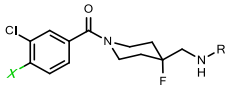

			5-HT_{1A} receptor bias factor (logarithmic value)					
Compd	**X**	**R**	**ERK1/2 vs. cAMP**	**ERK1/2 vs. β-arrestin**	**ERK1/2 vs. Ca^{2+}**	**cAMP vs. β-arrestin**	**cAMP vs. Ca^{2+}**	**β-arrestin vs. Ca^{2+}**
10	F	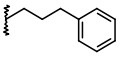	0.74	0.82	0.65	0.09	-0.09	-0.17
11	F	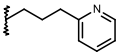	0.71	0.34	-0.09	-0.37	-0.80	-0.42
12	F	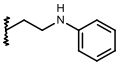	0.90	1.19	0.52	0.28	-0.38	-0.66
13	F	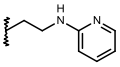	0.51	0.50	0.65	-0.01	0.15	0.15
14	F	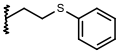	1.27	0.82	–[a]	-0.45	–	–
15	F	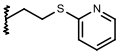	0.78	0.67	0.81	-0.12	0.03	0.15
16	F	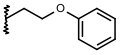	1.05	0.51	1.78	-0.54	0.73	1.27
17	F	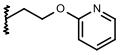	1.30	1.01	1.57	-0.30	0.27	0.57
19	Cl	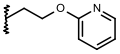	1.13	1.63	1.63	0.51	0.50	0.00
20	F	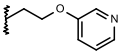	0.33	0.15	0.10	-0.18	-0.23	-0.05
22	F	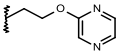	0.70	0.12	0.63	-0.58	-0.07	0.51
27	F	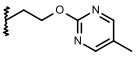	1.52	1.10	–	-0.42	–	–
1			1.17	1.02	1.76	-0.15	0.59	0.74
8-OH-DPAT			0.79	-0.39	–	-1.18	–	–
Buspirone			0.66	0.14	–	-0.52	–	–
Serotonin			0.00	0.00	0.00	0.00	0.00	0.00

[a]- no data for Ca^{2+} assay

In general, the novel series showed highest bias for ERK1/2 phosphorylation, especially vs. cAMP and Ca^{2+} (mean bias factors 0.91 and 0.83, respectively). The bias was most pronounced in the case of the aryloxyethanamine derivatives, where high preference (bias factors >1) was observed

in majority of cases. In this respect, the novel aryloxyethanamines were the most similar to the reference 5-HT_{1A} receptor biased agonist **1**, which previously showed preference for ERK1/2 phosphorylation, particularly over cAMP inhibiton.[27]

Noteworthy, as mentioned in the Introduction, it has been suggested that intensification of signal transduction through phosphorylation of ERK1/2 kinases may be important for antidepressant effects.[75–77] In fact, in post-mortem examinations of suicide victims with previously diagnosed depression, reduction of ERK1/2 expression and phosphorylation in brain structures was observed.[77,78] Furthermore, depression caused by chronic stress was found to be associated with ERK phosphorylation deficits,[79–82] and the chronic administration of ERK inhibitors caused anhedonia and anxiety behavior.[81] On the other hand, the inhibition of cAMP synthesis in the hippocampus resulting from the activation of the 5-HT_{1A} receptor may lead to reduced phosphorylation of the Ca^{2+}/calmodulin-dependent protein kinase II (CaMKII) and thus result in impairment of cognitive functions.[83] The above considerations further support the need for selective stimulation of a desired intracellular signaling in order to achieve optimal therapeutic benefit. In this context, the newly discovered aryloxyethyl derivatives of 1-(1-benzoylpiperidin-4-yl)methanamine represent a favorable extension of the prototype ERK1/2-preferring 5-HT_{1A} receptor biased agonist **1**, which is, so far, the sole representative of such a functional profile. The present study also evidenced clear difference in functional activity between these compounds and the widely used reference agonist 8-OH-DPAT and the partial agonist buspirone.

In vivo and *ex vivo* studies of the lead compound 17

Ex vivo ERK1/2 phosphorylation measurement

In view of the preferential activation of ERK1/2 phosphorylation *in vitro* by compound **17** and the key role of ERK1/2 phosphorylation for mediating antidepressant activity, we assessed the level of pERK1/2 in the rat prefrontal cortex (PFC) after oral administration of compound **17**. We found that compound **17** robustly and significantly increased rat PFC ERK1/2 phosphorylation in a time-dependent manner. The maximal increase of pERK1/2 level was observed after 15 min (T_{max}) and the statistically significant elevation of pERK1/2 was maintained also 30 min after administration (Figure 5A).

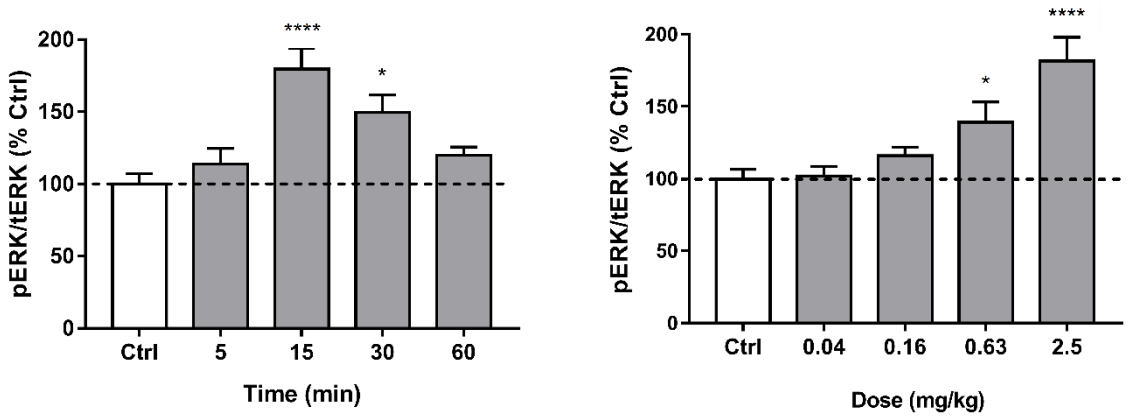

Figure 5A and **5B.** The effect of compound **17** on phospho-ERK1/2 (pERK1/2) and total-ERK 1/2 (tERK 1/2) levels in rat prefrontal cortex. A. time-course (5, 15, 30 and 60 min) of the effects induced by a single oral administration of compound **17** at a dose of 2.5 mg/kg or vehicle (water). B. dose-response of the effects of compound **17** tested at 15 min after administration. All samples were tested in duplicate, in two separate experiments. For normalization purposes, the value of phospho-ERK1/2 was divided by a corresponding value of total-ERK 1/2 for each sample, then the ratios were used for statistical analysis (time course: one-way ANOVA ($F(4,30)=10.87$; $p<0.0001$; dose-response: one-way ANOVA ($F(4,31)=10.19$; $p<0.0001$) followed by Bonferroni's post-hoc test). For graphical presentations, data are expressed as the mean ± SEM (2 measures for each of 6–8 rats per group), the mean value of the vehicle-treated group was set at 100% (control value) and all data were expressed as a percentage relative to the control value. *$p < 0.05$, ****$p < 0.0001$ compared to vehicle group.

Next, we investigated the dose-dependence of stimulation of ERK1/2 phosphorylation by compound **17** at the T_{max} after oral administration (see Pharmacokinetic studies below). Statistically significant elevation of pERK1/2 was observed at the two highest doses (2.5 mg/kg

and 0.63 mg/kg), but a tendency to increase pERK1/2 levels was also seen at lower doses (Figure 5B). These results are in agreement with the data obtained previously for selective agonists of 5-HT_{1A} receptors.[84]

Pharmacokinetic studies and PK/PD relationship

In order to establish the relationship between the pharmacodynamic effects of compound **17** and its exposure, we performed pharmacokinetic studies, including determination of concentrations of **17** in serum and brain of the rat. Both the time course and the dose-response profiles of ERK1/2 phosphorylation in PFC were found to correspond closely with the pharmacokinetic data. After oral administration we found the highest concentration of compound **17** in both serum and brain after 15 minutes (Figure 6). At this time point we also observed a dose-dependent increase in serum and brain concentration, with the highest concentrations produced by a dose of 2.5 mg/kg p.o. (Figure 7). Noteworthy, concentrations of compound **17** in brain tissue were higher than in serum for all doses.

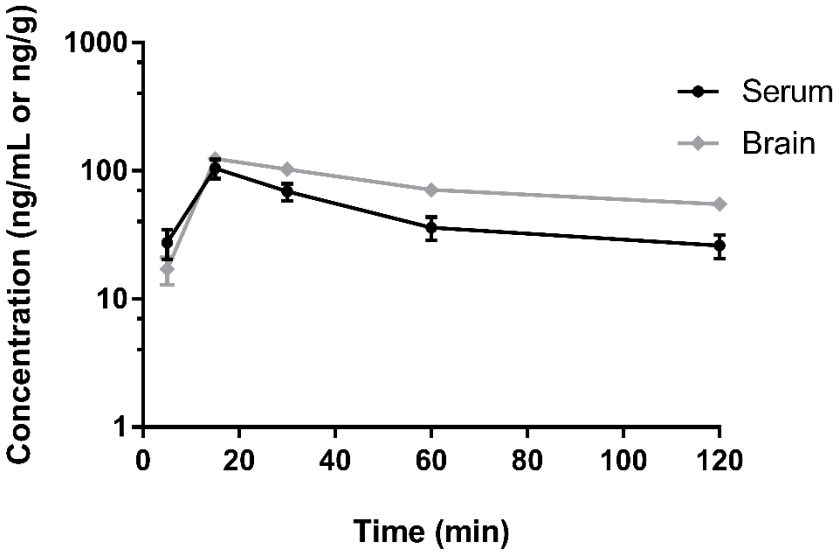

Figure 6. Serum and brain concentrations (mean ± SEM) of compound **17** following oral administration of a dose of 2.5 mg/kg to rats (n=6–8 animals per time point).

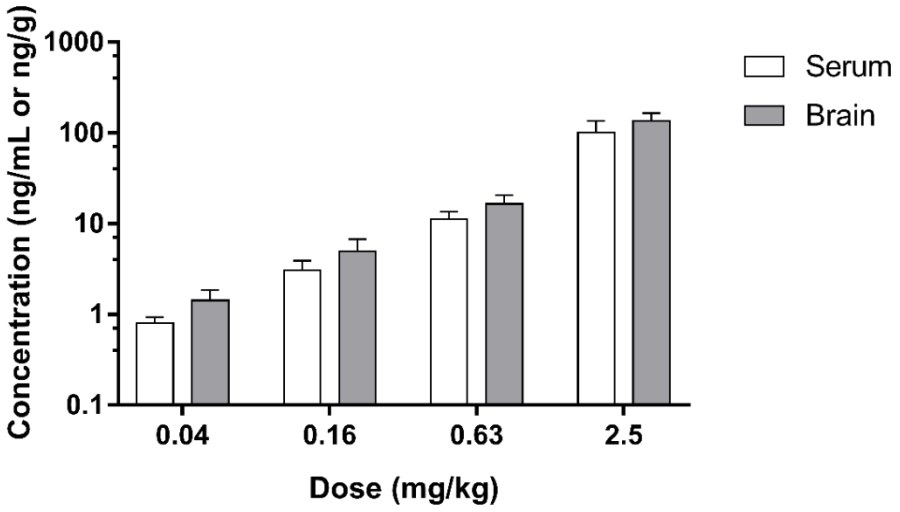

Figure 7. Dose-dependence in compound **17** serum and brain concentrations 15 min after oral administration to rats (each bar represents mean of 6–8 concentrations ± SEM).

To describe quantitatively the PK-PD relationship between ERK1/2 phosphorylation and serum drug concentration, a simple E_{max} model was applied in Phoenix WinNonlin v.7.0 (Certara Corp., USA). (Figure 8).

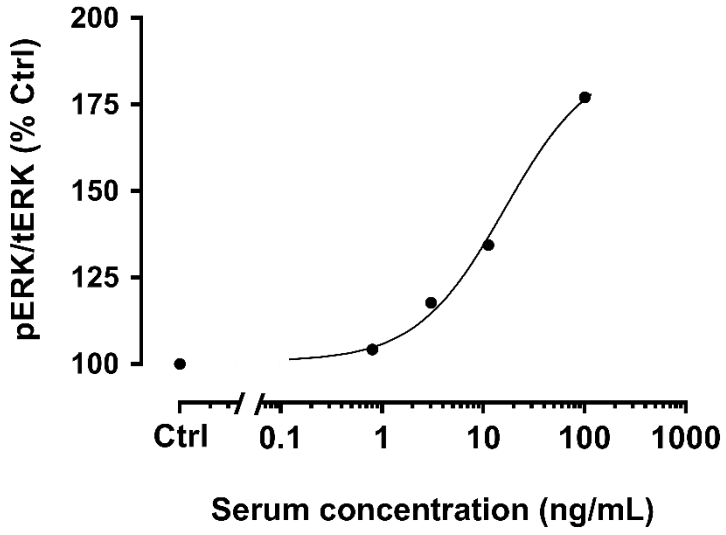

Figure 8. Observed (symbols) and pharmacodynamic model predicted (line) pERK/tERK ratio (normalized to the vehicle control) as a function of mean serum concentrations of compound **17**. ERK phosphorylation was measured 15 min following compound administration at four different oral doses (0.04, 0.16, 0.63, and 2.5 mg/kg) to rats (n=6-8 dose).

The proposed model captured the experimental data well with an estimated EC_{50} value (i.e. the serum concentration of **17** which elicits half-maximal pERK response) of 17.20 ng/mL. These results point to a clear PK/PD relationship between drug concentrations of **17** and its induction of pERK1/2 phosphorylation in rat prefrontal cortex.

In order to assess rat pharmacokinetic parameters of **17**, serum concentration versus time data following oral administration were analyzed by a non-compartmental approach. Compound **17** (2.5 mg/kg p.o.) was rapidly absorbed from the gastrointestinal tract (T_{max} = 15 min) and reached relatively high serum concentrations (C_{max} = 104.7 ng/mL). Brain levels followed exactly the same pattern with C_{max} of 124.4 ng/g. The area under the concentration-time curve from the time of dosing to infinity ($AUC_{0-\infty}$) was 8962.3 ng·min/L and 16834.2 ng·min/g for serum and brain, respectively. The apparent volume of distribution (V_z/F) during terminal phase was 35.9 L/kg. The studied compound was also characterized by a favourable value of serum elimination half-life ($t_{0.5\lambda z}$) of 89.3 min. The value of this parameter for brain tissue was even higher and it was 104.9 min.

Antidepressant-like activity

Compound **17** was tested in the rat forced swimming test (FST, Porsolt test), which is one of the most widely used procedures to evaluate antidepressant-like activity.[85,86] Given that the T_{max} for serum and brain exposure was observed at 15 min, which also corresponds to the time-point for highest ERK1/2 phosphorylation, we investigated the antidepressant activity of compound **17** using this pretreatment time. Compound **17** showed potent activity (minimal effective dose 0.16 mg/kg p.o.) and exhibited a very strong effect, completely abolishing immobility at a dose of 2.5 mg/kg p.o. (Figure 9, Supporting Information Table S4).

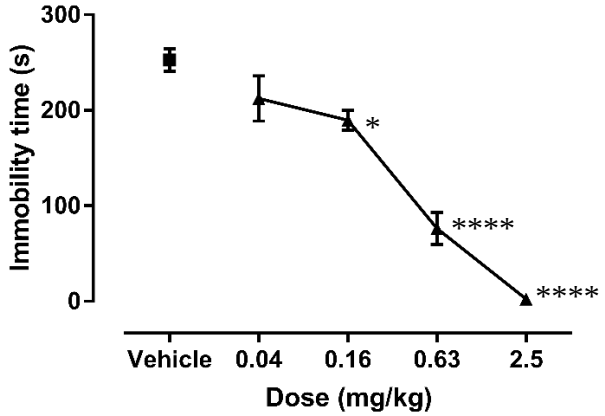

Figure 9. Antidepressant-like activity of compound **17** in the FST in rats (15 min pretreatment time). Values represent the mean ± SEM of the immobility time during 5-min test session compared to the vehicle group (one-way ANOVA ($F(4,29)=66.22$; $p<0.0000001$) followed by Bonferroni's post hoc test) *$p < 0.05$, ****$p < 0.00001$, n=6-8

In order to clarify the PK/PD relationship between the behavioral data (immobility time in the FST) and serum concentrations of compound **17**, the results of FST tests were plotted against mean serum concentrations measured at 15 min after dosing. As presented in Figure 10, the estimated concentration at which the compound exerts half of its maximal inhibitory effect (IC_{50}) was 6.76 ng/mL and was comparable to the EC_{50} value obtained for the activation of ERK1/2 phosphorylation in PFC by compound **17** (see above).

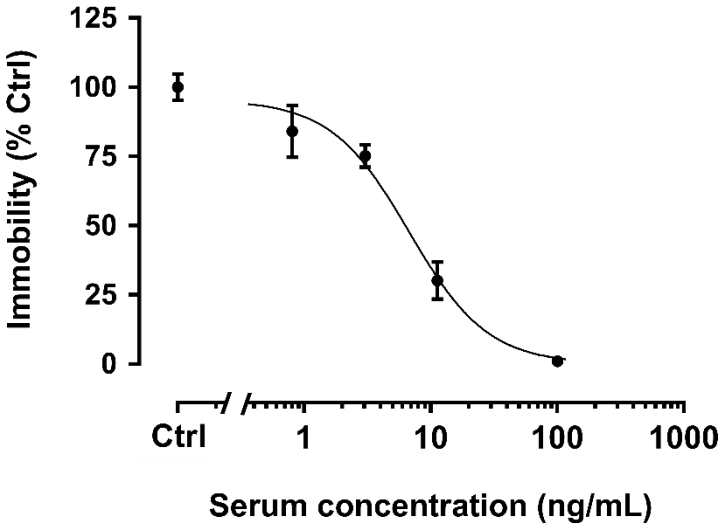

Figure 10. Observed (symbols) and pharmacodynamic model predicted (lines) immobility times (normalized to the vehicle control) as a function of mean serum concentrations of compound **17**. FST was performed 15 min following compound administration at four different oral doses (0.04, 0.16, 0.63, and 2.5 mg/kg) to rats (n=6-8 dose).

The activity of compound **17** in the FST was also evaluated 60 min after oral administration, which is a standard pretreatment time used in this type of experiments. The obtained results are very similar to those obtained with a 15 min pre-administration time, in both the effective dose range (MED = 0.16 mg/kg, ED_{50} = 0.3 mg/kg) and the maximal effect size (total immobility reduction at a dose of 2.5 mg/kg; Figure 9, Table S4). It is noteworthy that the antidepressant-like effect of **17** was maintained at 60 min, even though its concentrations in serum and brain, as well as pERK1/2 levels were decreased, thus suggesting a protracted behavioral effect of the compound. This observation is also in line with the previous studies of 5-HT_{1A} receptor biased agonists.[87] The antidepressant-like effect of compound **17** in the FST at 60 min was fully reversed by co-administration of the selective 5-HT_{1A} receptor antagonist WAY-100635 (0.63 mg/kg s.c.) and was not accompanied by any significant change in the locomotor activity, thus testifying to its specificity and a full 5-HT_{1A} receptor dependence. Moreover, at the doses tested (0.04 to 2.5 mg/kg p.o.), compound **17** did not elicit flat body posture (FBP), a common side effect of the 5-HT_{1A}

receptor stimulation, suggesting that its preference for activation of 5-HT_{1A} receptor-mediated ERK1/2 phosphorylation *in vitro* translates to preferential antidepressant effects rather than induction of 'behavioral syndrome' [31] (Table 7).

Table 7. Behavioral effects of compound **17** and references in the forced swimming test (FST) and serotonergic behavior – flat body posture (FBP) (60 min. after p.o. administration).

		Forced swimming test (FST, Porsolt test)			FBP[c]
Compd	Route of administration	Dose range (mg/kg)	MED[a] (mg/kg)	MaxED[b] (mg/kg)	MED (mg/kg)
17	p.o.	0.04–5	0.16	2.5	n.s.[d]
1[32]	p.o.	0.04–5	0.63	5	n.s.
8-OH-DPAT[32]	s.c.	0.04–0.63	0.16	–[e]	0.63
buspirone[32]	p.o.	0.16–2.5	n.s.	–[e]	n.s.
imipramine[88]	i.p.	3–10	10	–[e]	n.t.[f]
ketamine[89]	i.p.	5–15	5	–[e]	n.t.

[a] minimal effective dose; [b] The first dose at which the effects are maximal (total reduction of immobility time); [c] Flat body posture; [d] not significant; [e] maximal effect was not achieved (8-OH-DPAT 90% at 0.63 mg/kg, ketamine 43% at 15 mg/kg, imipramine 25% at 10 mg/kg); [f] not tested

Such activity, especially in terms of potency and maximal effect size, is very rare and was previously observed for the 5-HT_{1A} receptor biased agonist, **1**.[27,32] Thus, the present results further demonstrate consistence of the pharmacological effects of compound **17** with those of the reference biased agonist and suggest a high therapeutic potential of the novel compounds. Noteworthy, both ERK1/2 phosphorylation-preferring biased agonists (**17** and **1**) clearly outperformed all the reference compounds in terms of potency, maximal effect, lack of side effect (FBP) and oral activity (Table 7).

Moreover, under present conditions compound **17** was even more potent than **1** for reduction of immobility, showing activity at four times lower dose.[32] The potency of compound **17** after oral administration implies favorable gastrointestinal tract absorption and high penetration into the

central nervous system. Such observations support the predicted good developability profile of compound **17** as well as the overall "drug-likeness" of the novel series.

CONCLUSIONS

Recently, it was found that the rapid-acting antidepressant activity of ketamine is mediated by frontal cortex 5-HT_{1A} receptors and requires stimulation of ERK1/2 phosphorylation. Together with the previous findings on the role of ERK1/2 phosphorylation in mood control, it can be inferred that direct agonist activation of frontocortical 5-HT_{1A} receptor signaling by biased agonists offers the prospect of achieving beneficial therapeutic effects on mood without eliciting the dissociative and cognition-disrupting side effects which are seen with ketamine. Study of the first functionally-selective agonist of 5-HT_{1A} receptors, **1**, which preferentially activates ERK1/2 phosphorylation, confirmed that biased agonists may offer beneficial therapeutic effects on mood with reduced unwanted effects. However, to date, **1** was 'one of a kind' and there were no SAR studies that would lay a foundation for further development of 5-HT_{1A} receptor biased agonists. In the present study we therefore characterized a group of selective 5-HT_{1A} receptor agonists and carried out comprehensive analyses of structure-functional activity relationships. These allowed us to identify the aryloxyethanamine derivatives as the most biased agonists for ERK1/2 phosphorylation vs. cAMP and Ca^{2+}. Based on all data collected, we selected compound **17**, characterized by exceptional affinity (pK_i = 10.19), preference for ERK1/2 phosphorylation and favorable results of *in silico* predictions of drug-like properties (including CNS MPO and LELP). The results of SafetyScreen44™ Panel and other antitargets, the Bioavailability Panel, as well as CYP3A4, CYP2D6 and P-glycoprotein (Pgp) inhibition assays revealed its excellent overall selectivity and ADME properties, as well as relatively low drug–drug interaction potential. Finally, compound **17** stimulated ERK1/2 phosphorylation in rat cortex and outperformed **1** *in vivo*,

displaying robust antidepressant-like activity in Porsolt test at 0.16 mg/kg p.o. and a total reduction of immobility at 2.5 mg/kg p.o. Moreover, this effect was not accompanied by flat body posture, an observation that confirmed the compound's preference for activation of 5-HT_{1A} receptor signaling pathways that mediate therapeutic-like responses rather than those that mediate side effects. The new chemical scaffold presented herein, represented by compound **17** (also known as NLX-204), is not only a versatile tool for medicinal chemistry and further exploration of the target but also for drug development. Taken together, these results suggest that compounds in this chemical series may constitute promising candidates for development as novel treatments for mood disorders.

EXPERIMENTAL SECTION

Molecular modeling

Computer-aided ligand design and further studies on structure-activity relationships were based on ligand-receptor interactions analysis. In order to capture distinctive binding mode of a variety of functionally selective ligands, the general procedure for developing ligand-optimized models [90] was adopted in the present studies, regarding induced-fit technique as both protein binding site optimization method (in terms of amino acid side chains) and routine docking approach. The previously built pre-optimized serotonin 5-HT_{1A} receptor homology model [38] served as structural basis for ligand-steered side chain optimization.

In general, the 5-HT_{1B} crystal structure (PDB ID 4IAR) [91] was taken as a template for homology modeling. The alignment of amino acid sequences of the 5-HT_{1A} (UniProt database ID: P08908) and 5-HT_{1B} receptors was implemented from hhsearch model via GeneSilico Metaserver [92], which established the overall amino acid sequence identity for 38%. The basic 5-HT_{1A} receptor homology model was obtained via SwissModel platform.[93] Then it was validated by processing in Protein Preparation Wizard. Structure optimization stage, which was performed using induced-fit docking (IFD) [94] resulted in distinct protein-ligand complexes, which were subjected for visual inspection. Glide SP flexible docking procedure using OPLS3 force field was set for the IFD. H-bond constraint, as well as centroid of a grid box for docking to 5-HT_{1A} receptor were located on Asp3.32. Ligand structures were sketched in Maestro 2D Sketcher and optimized using LigPrep tool. Induced fit docking, LigPrep, Maestro and Protein Preparation Wizard were implemented in Small-Molecule Drug Discovery Suite (Schrödinger, Inc. New York, USA), which was licensed for Jagiellonian University Medical College.

Synthesis

General chemistry information

All the reagents were purchased from commercial suppliers (Sigma-Aldrich, Merck, Chempur, Fluorochem, Enamine, Acros Organics, Manchester Organics, POCh, Activate Scientific, Chem-impex International, Apollo Scientific) and were used without further purification. Analytical thin-layer chromatography (TLC) was performed on Merck Kieselgel 60 F_{254} (0.25 mm) pre-coated aluminum sheets (Merck, Darmstadt, Germany). Compounds were visualized with UV light and by suitable visualization reagents (2.9% solution of ninhydrin in mixture of 1-propanol and acetic acid (100/3, v/v) and Pancaldi reagent (solution of 12.0 g $(NH_4)_6Mo_7O_{24}$, 0.5 g $Ce(SO_4)_2$ and 6.8 mL of 98% H_2SO_4 in 240 mL of water). Flash chromatography was performed on CombiFlash RF (Teledyne Isco), using disposable silica gel flash columns RediSep Rf (silica gel 60, particle size 40–63 μm) and RediSep Gold (silica gel 60, particle size 20–40 μm) purchased from Teledyne Isco. The microwave reactions were conducted in a Discover LabMate (CEM Corporation). The UPLC-MS or UPLC-MS/MS analyses were done on UPLC-MS/MS system comprising Waters ACQUITY UPLC (Waters Corporation, Milford, MA, USA) coupled with Waters TQD mass spectrometer (electrospray ionization mode ESI with tandem quadrupole). Chromatographic separations were carried out using the ACQUITY UPLC BEH (bridged ethyl hybrid) C18 column: 2.1 × 100 mm and 1.7 μm particle size. The column was maintained at 40 °C and eluted under gradient conditions using 95% to 0% of eluent A over 10 min, at a flow rate of 0.3 mL/min. Eluent A: 0.1% solution of formic acid in water (v/v); eluent B: 0.1% solution of formic acid in acetonitrile (v/v). A total of 10 μL of each sample was injected, and chromatograms were recorded using Waters eλ PDA detector. The spectra were analysed in the range of 200–700 nm with 1.2 nm resolution and at a sampling rate of 20 points/s. The UPLC/MS purity of all the test compounds

and key intermediates were determined to be >95%. ^{1}H NMR, ^{13}C NMR, and ^{19}F NMR spectra were obtained in a Varian Mercury spectrometer (Varian Inc., Palo Alto, CA, USA), in $CDCl_3$, CD_3OD or DMSO-d_6 operating at 300 MHz (^{1}H NMR), 75 MHz (^{13}C NMR), and 282 MHz (^{19}F NMR). Chemical shifts are reported as δ values (ppm) relative to TMS δ = 0 (^{1}H) as internal standard. The *J* values are expressed in Hertz (Hz). Signal multiplicities are represented by the following abbreviations: s (singlet), br s (broad singlet), bd (broad dublet), d (doublet), dd (doublet of doublets), dt (doublet of triplets), t (triplet), td (triplet of doublets), tdd (triplet of doublet of doublets), q (quartet), dq (doublet of quartets), m (multiplet). Elemental analyses were conducted using a Vario EL III elemental analyser (elementar Analysensystem GmbH). Melting points were determined on Büchi Melting Point B-540 apparatus using open glass capillaries and are uncorrected.

Synthetic procedures

General procedure for the synthesis of benzoylpiperidin-4-one derivatives (4, 5)

4-Piperidone hydrochloride monohydrate (1.0 equiv) was dissolved in a mixture of dry DCM and Et_3N and cooled to 0 °C. The appropriate benzoyl chloride **2** or **3** (1.1 equiv) was added dropwise. The reaction mixture was subsequently warmed to room temperature and stirred for 12 h. The solvent was removed in vacuo, residue was washed with a mixture of 1.0 M HCl and water (1:1) (30 mL), and extracted with DCM. Organic layers were dried over magnesium sulfate, filtered and concentrated in vacuo. The crude product was purified by flash chromatography.

1-(3-Chloro-4-fluorobenzoyl)piperidin-4-one (4)

Compound **4** was prepared using 4-piperidone hydrochloride monohydrate (7.500 g, 49.02 mmol), 3-chloro-4-fluorobenzoyl chloride (**2**) (10.407 g, 53.92 mmol), Et_3N (25 mL) in DCM (125 mL).

Purification: *n*-hexane/EtOAc (6/4, v/v). Yield: 60 %; cream-colored crystallizing oil. ^{1}H NMR (300 MHz, $CDCl_3$, δ): 7.56 (dd, *J* = 2.1, 6.9 Hz, 1H), 7.37 (ddd, *J* = 2.2, 4.6, 8.4 Hz, 1H), 7.25–7.17 (m, 1H), 3.87 (br s, 4H), 2.51 (br s, 4H). ^{19}F NMR (282 MHz, $CDCl_3$, δ): -111.5 (s, 1F). Formula: $C_{12}H_{11}ClFNO_2$; MS (ESI^+): *m/z* 256 [$M+H^+$].

1-(3,4-Dichlorobenzoyl)piperidin-4-one (5)

Compound **5** was prepared using 4-piperidone hydrochloride monohydrate (4.000 g, 29.63 mmol), 3,4-dichlorobenzoyl chloride (**3**) (6.828 g, 32.59 mmol), Et_3N (30 mL) in DCM (100 mL). Purification: *n*-hexane/EtOAc (5/5, v/v). Yield: 47%; pale yellow crystallizing oil. ^{1}H NMR (300 MHz, $CDCl_3$, δ):7.58 (d, *J* = 1.8 Hz, 1H), 7.52 (d, *J* = 8.2 Hz, 1H), 7.31 (dd, *J* = 2.1, 8.2 Hz, 1H), 3.86 (br s, 4H), 2.51 (br s, 4H). Formula: $C_{12}H_{11}Cl_2NO_2$; MS (ESI^+): *m/z* 272 [$M+H^+$].

General procedure for the synthesis of benzoyl-1-oxa-6-azaspiro[2.5]octane-2-carbonitrile derivatives (6, 7)

To the benzoylpiperidin-4-one derivative **4** or **5** (1.00 equiv) and tetrabutylammonium bromide (0.04 equiv) dissolved in DCM and 30% aqueous solution of NaOH, chloroacetonitrile (1.40 equiv) was added dropwise. The mixture was stirred at room temperature for 2 hours and then quenched with a saturated, aqueous solution of sodium bicarbonate. Next, the mixture was extracted with DCM, dried over magnesium sulfate, filtered and concentrated in vacuo. The obtained crude brown oil was purified by flash chromatography to yield pure product.

6-(3-Chloro-4-fluorobenzoyl)-1-oxa-6-azaspiro[2.5]octane-2-carbonitrile (6)

Compound **6** was prepared using 1-(3-chloro-4-fluorobenzoyl)piperidin-4-one (**4**) (7.050 g, 27.67 mmol), tetrabutylammonium bromide (0.356 g, 1.11 mmol), chloroacetonitrile (2.44 mL, 38.71 mmol), and 30% aqueous solution of NaOH (19 mL) in DCM (47 mL). Purification: DCM/Et_2O

(7/3, v/v). Yield: 80%; pale yellow crystallizing oil. ^{1}H NMR (300 MHz, $CDCl_3$, δ): 7.52 (dd, *J* = 2.1, 6.7 Hz, 1H), 7.38–7.29 (m, 1H), 7.24–7.14 (m, 1H), 4.35–3.70 (m, 2H), 3.67–3.49 (m, 2H), 3.41 (s, 1H), 2.20–1.69 (m, 4H). Formula: $C_{14}H_{12}ClFN_2O_2$; MS (ESI^+): *m/z* 295 [$M+H^+$].

6-(3,4-Dichlorobenzoyl)-1-oxa-6-azaspiro[2.5]octane-2-carbonitrile (7)

Compound **7** was prepared using 1-(3,4-dichlorobenzoyl)piperidin-4-one (**5**) (3.405 g, 12.52 mmol), tetrabutylammonium bromide (0.161 g, 0.50 mmol), chloroacetonitrile (1.11 mL, 17.53 mmol), and 30% aqueous solution of NaOH (8.6 mL) in DCM (21 mL). Purification: $EtOAc/Et_2O/NH_{3(aq)}$ (8.5/1.5/0.02, v/v/v). Yield: 87%; yellow crystallizing oil. ^{1}H NMR (300 MHz, $CDCl_3$, δ): 7.59–7.45 (m, 2H), 7.31–7.19 (m, 1H), 4.44–4.15 (m, 1H), 3.82–3.49 (m, 3H), 3.41 (s, 1H), 1.99–1.37 (m, 4H). ^{13}C NMR (75 MHz, $CDCl_3$, δ): 168.2, 134.9, 134.6, 133.2, 130.8, 129.2, 126.2, 115.2, 63.1, 47.1, 45.8, 40.8, 32.6, 31.1. Formula: $C_{14}H_{12}Cl_2N_2O_2$; MS (ESI^+): *m/z* 311 [$M+H^+$].

General procedure for the synthesis of cyanohydrine derivatives (8, 9)

To the appropriate nitrile **6** or **7** (1.0 equiv) dissolved in dry dichloromethane at -10 °C in a round bottom teflon flask, 70% solution of HF in pyridine (40.0 equiv) was added dropwise and the mixture was stirred at room temperature for 24–36 hours. The mixture was then slowly quenched with 10% aqueous solution of potassium carbonate to pH 9, diluted with brine and extracted with EtOAc. The combined organic layers were dried over magnesium sulfate, filtered and concentrated in vacuo. Purification by flash chromatography yielded pure product.

2-(1-(3-Chloro-4-fluorobenzoyl)-4-fluoropiperidin-4-yl)-2-hydroxyacetonitrile (8)

Compound **8** was prepared using 6-(3-chloro-4-fluorobenzoyl)-1-oxa-6-azaspiro[2.5]octane-2-carbonitrile (**6**) (3.450 g, 11.74 mmol), 70% solution of HF in pyridine (12.1 mL, 466.40 mmol)

in DCM (23 mL). Purification: *n*-hexane/DCM/methanol/$NH_{3(aq)}$ (6/3.5/0.5/0.02, v/v/v/v). Yield: 54%; yellow crystallizing oil. ^{1}H NMR (300 MHz, $CDCl_3$, δ): 7.49 (dd, *J* = 2.1, 6.7 Hz, 1H), 7.34–7.27 (m, 1H), 7.24–7.17 (m, 1H), 4.65 (br s, 1H), 4.40 (d, *J* = 12.6 Hz, 1H), 3.75 (br s, 1H), 3.51–3.03 (m, 2H), 2.19–1.65 (m, 4H), O*H* proton not detected. ^{19}F NMR (282 MHz, $CDCl_3$, δ): -111.6 (s, 1F), -170.7 (s, 1F). ^{13}C NMR (75 MHz, $CDCl_3$, δ): 168.5, 159.1 (d, *J* = 254 Hz), 132.0 (d, *J* = 4.4 Hz), 129.8, 127.1 (d, *J* = 7.7 Hz), 121.8 (d, *J* = 18.2 Hz), 117.0 (d, *J* = 22 Hz), 116.6 (d, *J* = 2.8 Hz), 93.3 (d, *J* = 181.8 Hz), 66.7 (d, *J* = 28.2 Hz), 42.8, 37.9, 31.4, 30.3. Formula: $C_{14}H_{13}ClF_2N_2O_2$; MS (ESI^+): *m/z* 315 [$M+H^+$].

2-(1-(3,4-Dichlorobenzoyl)-4-fluoropiperidin-4-yl)-2-hydroxyacetonitrile (9)

Compound **9** was prepared using 6-(3,4-dichlorobenzoyl)-1-oxa-6-azaspiro[2.5]octane-2-carbonitrile (**7**) (3.300 g, 10.61 mmol), 70% solution of HF in pyridine (11.5 mL, 424.44 mmol) in DCM (16 mL). Purification: *n*-hexane/DCM/methanol/$NH_{3(aq)}$ (6/3.5/0.5/0.02, v/v/v/v). Yield: 68%; yellow crystallizing oil. ^{1}H NMR (300 MHz, $CDCl_3$, δ): 7.55–7.47 (m, 2H), 7.26–7.20 (m, 1H), 4.61 (br s, 1H), 4.39 (d, *J* = 12.1 Hz, 1H), 3.83–3.61 (m, 1H), 3.45–3.06 (m, 2H), 1.79 (br s, 4H), O*H* proton not detected. ^{19}F NMR (282 MHz, $CDCl_3$, δ): -170.8 (s, 1F). Formula: $C_{14}H_{13}Cl_2F_1N_2O_2$; MS ($ESI^+$): *m/z* 331 [$M+H^+$].

General procedures for the preparation of 1-(1-benzoylpiperidin-4-yl)methanamine derivatives (10–27).

To appropriate cyanohydrin (**8** or **9**) (1.0 equiv) dissolved in methanol, DABCO (2.0–12.5 equiv) was added in one portion, followed by the appropriate amine (1.0–1.6 equiv), 4Å molecular sieves, sodium cyanoborohydride (1.6–7.8 equiv), and iron sulfate heptahydrate ($FeSO_4 \times 7\ H_2O$) (1.1 equiv). The mixture was stirred at room temperature until the cyanohydrin was consumed (24–72

h). After that time, the reaction mixture was filtered, concentrated in vacuo and next brine was added. The resulting mixture was extracted with EtOAc (three times), organics were combined and dried over magnesium sulfate, filtered and concentrated. The crude product was purified by flash chromatography.

(3-Chloro-4-fluorophenyl)(4-fluoro-4-(((3-phenylpropyl)amino)methyl)piperidin-1-yl)methanone (10)

The title compound was prepared using 2-(1-(3-chloro-4-fluorobenzoyl)-4-fluoropiperidin-4-yl)-2-hydroxyacetonitrile (**8**) (0.120 g, 0.38 mmol), 3-phenylpropan-1-amine (0.072 g, 0.54 mmol), DABCO (0.535 g, 4.78 mmol), sodium cyanoborohydride (0.187 g, 2.98 mmol), molecular sieves (0.900 g) and iron sulfate heptahydrate (0.117 g, 0.42 mmol) in methanol (5 mL). Purification: *n*-hexane/Et_2O/DCM/methanol/$NH_{3(aq)}$ (3/2/4.5/0.5/0.02, v/v/v/v/v). Yield: 41%; pale beige powder. ^{1}H NMR (300 MHz, $CDCl_3$, δ): 7.48 (dd, *J* = 2.3, 7.0 Hz, 1H), 7.34–7.23 (m, 3H), 7.22–7.10 (m, 4H), 4.50 (br s, 1H), 3.60 (d, *J* = 19.9 Hz, 1H), 3.46–3.08 (m, 2H), 2.80–2.60 (m, 6H), 2.09–1.90 (m, 2H), 1.87–1.45 (m, 5H). ^{13}C NMR (75 MHz, $CDCl_3$, δ): 168.0, 158.8 (d, *J* = 254 Hz), 142.0, 132.9 (d, *J* = 3.5 Hz), 129.7, 128.4 (2C), 128.3 (2C), 127.1 (d, *J* = 6.9 Hz), 125.8, 121.5 (d, *J* = 18.4 Hz), 116.8 (d, *J* = 22 Hz), 94.3 (d, *J* = 172 Hz), 57.5 (d, *J* = 22 Hz), 49.8, 43.6, 38.3, 33.5, 33.2, 32.7, 31.6. Formula: $C_{22}H_{25}ClF_2N_2O$; MS (ESI^+): *m/z* 407 [$M+H^+$]. Melting point: 62–64 °C.

(3-Chloro-4-fluorophenyl)(4-fluoro-4-(((3-(pyridin-2-yl)propyl)amino)methyl)piperidin-1-yl)methanone (11)

The title compound was prepared using 2-(1-(3-chloro-4-fluorobenzoyl)-4-fluoropiperidin-4-yl)-2-hydroxyacetonitrile (**8**) (0.100 g, 0.32 mmol), 3-(pyridin-2-yl)propan-1-amine (0.056 g, 0.41 mmol), DABCO (0.444 g, 3.97 mmol), sodium cyanoborohydride (0.155 g, 2.48 mmol), molecular sieves (0.900 g) and iron sulfate heptahydrate (0.097 g, 0.35 mmol) in methanol (5 mL).

Purification: *n*-hexane/EtOAc/methanol/$NH_{3(aq)}$ (2/7/1/0.02, v/v/v/v). Yield: 57%; orange oil. ^{1}H NMR (300 MHz, $CDCl_3$, δ): 8.53–8.43 (m, 1H), 7.57 (dt, *J* = 1.8, 7.6 Hz, 1H), 7.46 (dd, *J* = 1.8, 7.0 Hz, 1H), 7.32–7.24 (m, 1H), 7.21–7.04 (m, 3H), 4.47 (br s, 1H), 3.57 (br s, 1H), 3.44–3.05 (m, 2H), 2.80 (dd, *J* = 7.9, 15.5 Hz, 3H), 2.73–2.60 (m, 3H), 2.07–1.84 (m, 4H), 1.69 (br s, 3H). ^{19}F NMR (282 MHz, $CDCl_3$, δ): -112.7 (s, 1F), -166.6 (s, 1F). ^{13}C NMR (75 MHz, $CDCl_3$, δ): 168.0, 161.7, 158.7 (d, *J* = 254 Hz), 149.2, 136.3, 132.9 (d, *J* = 4.7 Hz), 129.7, 127.1 (d, *J* = 8.1 Hz), 122.8, 121.5 (d, *J* = 18.4 Hz), 121.0, 116.8 (d, *J* = 22 Hz), 94.3 (d, *J* = 172 Hz), 57.4 (d, *J* = 22 Hz), 49.8, 43.7, 38.2, 35.9, 33.6, 32.9, 29.9. Formula: $C_{21}H_{24}ClF_2N_3O$; MS (ESI^+): *m/z* 408 [$M+H^+$].

(3-Chloro-4-fluorophenyl)(4-fluoro-4-(((2-(phenylamino)ethyl)amino)methyl)piperidin-1-yl)methanone (12)

The title compound was prepared using 2-(1-(3-chloro-4-fluorobenzoyl)-4-fluoropiperidin-4-yl)-2-hydroxyacetonitrile (**8**) (0.144 g, 0.46 mmol), N^1-phenylethane-1,2-diamine (0.095 g, 0.55 mmol), DABCO (0.103 g, 0.92 mmol), sodium cyanoborohydride (0.046 g, 0.73 mmol), molecular sieves (0.900 g) and iron sulfate heptahydrate (0.140 g, 0.42 mmol) in methanol (5 mL). Purification: *n*-hexane/EtOAc/methanol/$NH_{3(aq)}$ (3/6.5/0.5/0.02, v/v/v/v). Yield: 35%; yellow oil. ^{1}H NMR (300 MHz, $CDCl_3$, δ): 7.48 (dd, *J* = 1.8, 7.0 Hz, 1H), 7.33–7.24 (m, 1H), 7.22–7.13 (m, 3H), 6.76–6.67 (m, 1H), 6.66–6.58 (m, 2H), 4.51 (br s, 1H), 3.60 (br s, 1H), 3.35 (d, *J* = 15.8 Hz, 1H), 3.24–3.17 (m, 2H), 3.17–3.02 (m, 1H), 2.91 (t, *J* = 5.6 Hz, 2H), 2.85–2.71 (m, 2H), 2.02 (br s, 3H), 1.84–1.41 (m, 3H). ^{13}C NMR (75 MHz, $CDCl_3$, δ): 168.1, 158.8 (d, *J* = 254 Hz), 148.3, 132.8 (d, *J* = 3.5 Hz), 129.7, 129.3 (2C), 127.1 (d, *J* = 6.9 Hz), 121.5 (d, *J* = 18.4 Hz), 117.6, 116.8 (d, *J* = 22 Hz), 113.0 (2C), 94.3 (d, *J* = 172 Hz), 57.0 (d, *J* = 22 Hz), 48.9, 43.6, 43.3, 38.2, 33.6,

32.8. Formula: $C_{21}H_{24}ClF_2N_3O$; MS (ESI^+): *m/z* 408 [$M+H^+$]; Anal. Calcd for: C: 61.84; H: 5.93; N: 10.30. Found: C: 62.85; H: 6.72; N: 9.09.

(3-Chloro-4-fluorophenyl)(4-fluoro-4-(((2-(pyridin-2-ylamino)ethyl)amino)methyl)piperidin-1-yl)methanone (13)

The title compound was prepared using 2-(1-(3-chloro-4-fluorobenzoyl)-4-fluoropiperidin-4-yl)-2-hydroxyacetonitrile (**8**) (0.120 g, 0.38 mmol), N^1-(pyridin-2-yl)ethane-1,2-diamine (0.079 g, 0.46 mmol), DABCO (0.085 g, 0.76 mmol), sodium cyanoborohydride (0.038 g, 0.61 mmol), molecular sieves (0.900 g) and iron sulfate heptahydrate (0.117 g, 0.42 mmol) in methanol (5 mL). Purification: EtOAc/methanol (9/1, v/v) and then DCM/methanol/$NH_{3(aq)}$ (9.5/0.5/0.02, v/v/v). Yield: 23%; orange oil. ^1H NMR (300 MHz, $CDCl_3$, δ): 8.08–8.00 (m, 1H), 7.47 (dd, *J* = 2.1, 6.7 Hz, 1H), 7.44–7.35 (m, 1H), 7.32–7.26 (m, 1H), 7.20–7.11 (m, 1H), 6.55 (dd, *J* = 5.3, 6.4 Hz, 1H), 6.39 (d, *J* = 8.2 Hz, 1H), 5.10 (br s, 1H), 4.48 (br s, 1H), 3.57 (br s, 1H), 3.40–3.08 (m, 4H), 3.00 (br s, 1H), 2.89 (t, *J* = 5.9 Hz, 2H), 2.78 (d, *J* = 1.0 Hz, 2H), 2.01 (s, 2H), 1.59 (d, *J* = 17.0 Hz, 2H). ^{19}F NMR (282 MHz, $CDCl_3$, δ): -112.6 (s, 1F), -166.7 (s, 1F). ^{13}C NMR (75 MHz, $CDCl_3$, δ): 168.1, 158.7, 158.8 (d, *J* = 251 Hz), 147.9, 137.5, 132.8 (d, *J* = 3.5 Hz), 129.7, 127.1 (d, *J* = 7.7 Hz), 121.5 (d, *J* = 18.4 Hz), 116.8 (d, *J* = 22 Hz), 112.9, 107.1, 94.3 (d, *J* = 172 Hz), 57.0 (d, *J* = 22 Hz), 49.1, 43.6, 41.5, 38.2, 33.6, 32.8. Formula: $C_{20}H_{23}ClF_2N_4O$; MS (ESI^+): *m/z* 409 [$M+H^+$].

(3-Chloro-4-fluorophenyl)(4-fluoro-4-(((2-(phenylthio)ethyl)amino)methyl)piperidin-1-yl)methanone (14)

The title compound was prepared using 2-(1-(3-chloro-4-fluorobenzoyl)-4-fluoropiperidin-4-yl)-2-hydroxyacetonitrile (**8**) (0.100 g, 0.32 mmol), 2-(phenylthio)ethanamine (0.063 g, 0.41 mmol), DABCO (0.446 g, 3.98 mmol), sodium cyanoborohydride (0.156 g, 2.48 mmol), molecular sieves

(0.800 g) and iron sulfate heptahydrate (0.097 g, 0.35 mmol) in methanol (5 mL). Purification: DCM/methanol/$NH_{3(aq)}$ (9.5/0.5/0.02, v/v/v). Yield: 59%; colorless oil. ^{1}H NMR (300 MHz, $CDCl_3$, δ): 7.48 (dd, *J* = 1.8, 7.0 Hz, 1H), 7.38–7.26 (m, 5H), 7.23–7.14 (m, 2H), 4.50 (br s, 1H), 3.59 (br s, 1H), 3.46–3.10 (m, 2H), 3.09–3.03 (m, 2H), 2.89–2.83 (m, 2H), 2.80–2.68 (m, 2H), 1.97 (br s, 2H), 1.69 (br s, 3H). ^{13}C NMR (75 MHz, $CDCl_3$, δ): 168.0, 158.8 (d, *J* = 252 Hz), 135.6, 132.9 (d, *J* = 4.4 Hz), 129.7, 129.0 (4C), 127.1 (d, *J* = 8.1 Hz), 126.3, 121.5 (d, *J* = 18.2 Hz), 116.8 (d, *J* = 22 Hz), 94.3 (d, *J* = 172 Hz), 56.9 (d, *J* = 22 Hz), 48.7, 43.7, 38.2, 34.2, 33.7, 32.7. Formula: $C_{21}H_{23}ClF_2N_2OS$; MS (ESI^+): *m/z* 425 [$M+H^+$].

(3-Chloro-4-fluorophenyl)(4-fluoro-4-(((2-(pyridin-2-ylthio)ethyl)amino)methyl)piperidin-1-yl)methanone (15)

The title compound was prepared using 2-(1-(3-chloro-4-fluorobenzoyl)-4-fluoropiperidin-4-yl)-2-hydroxyacetonitrile (**8**) (0.150 g, 0.48 mmol), 2-(pyridin-2-ylsulfanyl)ethanamine (0.145 g, 0.76 mmol), DABCO (0.669 g, 5.97 mmol), sodium cyanoborohydride (0.234 g, 3.73 mmol), molecular sieves (1.043 g) and iron sulfate heptahydrate (0.146 g, 0.53 mmol) in methanol (5 mL). Purification: *n*-hexane/EtOAc/methanol/$NH_{3(aq)}$ (8/1.5/0.5/0.02, v/v/v/v). Yield: 64%; pale yellow oil. ^{1}H NMR (300 MHz, $CDCl_3$, δ): 8.39 (td, *J* = 1.2, 5.5 Hz, 1H), 7.52–7.40 (m, 2H), 7.32–7.26 (m, 1H), 7.21–7.13 (m, 2H), 6.97 (ddd, *J* = 1.0, 5.0, 7.3 Hz, 1H), 4.50 (br s, 1H), 3.59 (br s, 1H), 3.41–3.07 (m, 4H), 2.96 (t, *J* = 6.4 Hz, 2H), 2.86–2.72 (m, 2H), 1.97 (br s, 2H), 1.63 (br s, 3H). ^{13}C NMR (75 MHz, $CDCl_3$, δ): 168.0, 158.4, 158.8 (d, *J* = 254 Hz), 149.4, 135.9, 132.9 (d, *J* = 4.4 Hz), 129.7, 127.1 (d, *J* = 7.7 Hz), 122.5, 121.5(d, *J* = 18.2 Hz), 119.5, 116.8 (d, *J* = 22 Hz), 94.3 (d, *J* = 172 Hz), 56.9 (d, *J* = 22 Hz), 49.4, 43.7, 38.2, 33.8, 32.7, 30.0. Formula: $C_{20}H_{22}ClF_2N_3OS$; MS (ESI^+): *m/z* 426 [$M+H^+$].

(3-Chloro-4-fluorophenyl)(4-fluoro-4-(((2-phenoxyethyl)amino)methyl)piperidin-1-yl)methanone (16)

The title compound was prepared using 2-(1-(3-chloro-4-fluorobenzoyl)-4-fluoropiperidin-4-yl)-2-hydroxyacetonitrile (**8**) (0.300 g, 0.96 mmol), 2-phenoxyethanamine (0.2 mL, 1.53 mmol), DABCO (1.36 g, 11.938 mmol), sodium cyanoborohydride (0.468 g, 7.45 mmol), molecular sieves (1.982 g) and iron sulfate heptahydrate (0.294 g, 1.06 mmol) in methanol (9 mL). Purification: *n*-hexane/EtOAc/methanol/$NH_{3(aq)}$ (6/3.5/0.5/0.02, v/v/v/v). Yield: 61%; beige crystallizing oil. ^{1}H NMR (300 MHz, $CDCl_3$, δ): 7.48 (dd, *J* = 2.1, 7.2 Hz, 1H), 7.33–7.26 (m, 3H), 7.22–7.13 (m, 1H), 6.99–6.86 (m, 3H), 4.51 (br s, 1H), 4.07 (t, *J* = 5.1 Hz, 2H), 3.71–3.53 (m, 1H), 3.22 (br s, 2H), 3.03 (t, *J* = 5.1 Hz, 2H), 2.92–2.77 (m, 2H), 2.01 (br s, 2H), 1.67 (br s, 3H). ^{19}F NMR (282 MHz, $CDCl_3$, δ): -112.6 (s, 1F), -166.5 (s, 1F). ^{13}C NMR (75 MHz, $CDCl_3$, δ): 168.1, 158.7 (d, *J* = 254 Hz), 158.7, 132.9 (d, *J* = 4 Hz), 129.7, 129.5 (2C), 127.1 (d, *J* = 7.2 Hz), 121.5 (d, *J* = 18.2 Hz), 120.9, 116.8 (d, *J* = 22 Hz), 114.5 (2C), 94.4 (d, *J* = 172 Hz), 67.2, 57.3 (d, *J* = 22 Hz), 49.3, 43.8, 38.3, 33.3, 31.1. Formula: $C_{21}H_{23}ClF_2N_2O_2$; MS (ESI^+): *m/z* 409 [$M+H^+$]; Anal. Calcd for: C: 61.69; H: 5.67; N: 6.85. Found: C: 61.95; H: 6.06; N: 6.44.

(3-Chloro-4-fluorophenyl)(4-fluoro-4-(((2-(pyridin-2-yloxy)ethyl)amino)methyl)piperidin-1-yl)methanone (17)

The title compound was prepared using 2-(1-(3-chloro-4-fluorobenzoyl)-4-fluoropiperidin-4-yl)-2-hydroxyacetonitrile (**8**) (0.220 g, 0.70 mmol), 2-(pyridin-2-yloxy)ethanamine (0.135 g, 0.98 mmol), DABCO (0.981 g, 8.76 mmol), sodium cyanoborohydride (0.343 g, 5.47 mmol), molecular sieves (1.043 g) and iron sulfate heptahydrate (0.214 g, 0.77 mmol) in methanol (5 mL). Purification: *n*-hexane/EtOAc/methanol/$NH_{3(aq)}$ (3/6.5/0.5/0.02, v/v/v/v). Yield: 53%; white crystallizing oil. ^{1}H NMR (300 MHz, $CDCl_3$, δ): 8.16–8.08 (m, 1H), 7.61–7.52 (m, 1H), 7.47 (dd,

J = 1.8, 7.0 Hz, 1H), 7.33–7.26 (m, 1H), 7.20–7.12 (m, 1H), 6.90–6.82 (m, 1H), 6.77–6.68 (m, 1H), 4.50 (br s, 1H), 4.42–4.33 (m, 2H), 3.57 (br s, 1H), 3.46–3.06 (m, 2H), 3.02 (t, *J* = 5.3 Hz, 2H), 2.91–2.73 (m, 2H), 2.01 (br s, 2H), 1.87–1.52 (m, 3H). ^{19}F NMR (282 MHz, $CDCl_3$, δ): -112.6 (s, 1F), -166.5 (s, 1F). ^{13}C NMR (75 MHz, $CDCl_3$, δ): 168.0, 163.6, 158.8 (d, *J* = 254 Hz), 146.8, 136.6, 132.9 (d, *J* = 4.6 Hz), 129.7, 127.1 (d, *J* = 7.7 Hz), 121.5 (d, *J* = 18.4 Hz), 116.9, 116.8 (d, *J* = 21 Hz), 111.0, 94.4 (d, *J* = 172 Hz), 65.1, 57.2 (d, *J* = 22 Hz), 49.2, 43.7, 38.4, 33.6, 32.8. Formula: $C_{20}H_{22}ClF_2N_3O_2$; MS (ESI^+): *m/z* 410 [$M+H^+$].

(3,4-Dichlorophenyl)(4-fluoro-4-(((2-phenoxyethyl)amino)methyl)piperidin-1-yl)methanone (18)

The title compound was prepared using 2-(1-(3,4-dichlorobenzoyl)-4-fluoropiperidin-4-yl)-2-hydroxyacetonitrile (**9**) (0.150 g, 0.45 mmol), 2-phenoxyethanamine (0.056 g, 0.41 mmol), DABCO (0.634 g, 5.66 mmol), sodium cyanoborohydride (0.034 g, 0.54 mmol), molecular sieves (0.500 g) and iron sulfate heptahydrate (0.137 g, 0.50 mmol) in methanol (8 mL). Purification: *n*-hexane/Et_2O/DCM/methanol/$NH_{3(aq)}$ (2/2/5.5/0.5/0.02, v/v/v/v/v). Yield: 44%; yellow oil. ^{1}H NMR (300 MHz, $CDCl_3$, δ): 7.54–7.45 (m, 2H), 7.33–7.26 (m, 2H), 7.23 (dd, *J* = 2.1, 8.2 Hz, 1H), 7.00–6.86 (m, 3H), 4.52 (br s, 1H), 4.07 (t, *J* = 5.1 Hz, 2H), 3.58 (br s, 1H), 3.44–3.10 (m, 2H), 3.03 (t, *J* = 5.1 Hz, 2H), 2.91–2.78 (m, 2H), 2.02 (br s, 2H), 1.61 (s, 3H). ^{13}C NMR (75 MHz, $CDCl_3$, δ): 167.9, 158.7, 135.7, 134.1, 133.0, 130.6, 129.5 (2C), 129.1, 126.2, 120.9, 114.5 (2C), 94.3 (d, *J* = 172 Hz), 67.2, 57.3 (d, *J* = 22 Hz), 49.3, 43.6, 38.2, 33.7, 32.7. Formula: $C_{21}H_{23}Cl_2FN_2O_2$; MS (ESI^+): *m/z* 425 [$M+H^+$].

(3,4-Dichlorophenyl)(4-fluoro-4-(((2-(pyridin-2-yloxy)ethyl)amino)methyl)piperidin-1-yl)methanone (19)

The title compound was prepared using 2-(1-(3,4-dichlorobenzoyl)-4-fluoropiperidin-4-yl)-2-hydroxyacetonitrile (**9**) (0.150 g, 0.45 mmol), 2-(pyridin-2-yloxy)ethanamine (0.081 g, 0.59 mmol), DABCO (0.634 g, 5.66 mmol), sodium cyanoborohydride (0.222 g, 3.53 mmol), molecular sieves (0.900 g) and iron sulfate heptahydrate (0.137 g, 0.50 mmol) in methanol (5 mL). Purification: EtOAc/methanol (9.5/0.5/, v/v). Yield: 41%; yellow oil. ^{1}H NMR (300 MHz, $CDCl_3$, δ): 8.17–8.08 (m, 1H), 7.61–7.53 (m, 1H), 7.52–7.44 (m, 2H), 7.23 (dd, *J* = 1.8, 8.2 Hz, 1H), 6.91–6.82 (m, 1H), 6.77–6.69 (m, 1H), 4.50 (br s, 1H), 4.43–4.34 (m, 2H), 3.71–3.47 (m, 1H), 3.47–3.07 (m, 2H), 3.03 (t, *J* = 5.3 Hz, 2H), 2.84 (d, *J* = 1.0 Hz, 2H), 2.00 (br s, 2H), 1.61 (br s, 3H). ^{19}F NMR (282 MHz, $CDCl_3$, δ): -166.6 (s, 1F). ^{13}C NMR (75 MHz, $CDCl_3$, δ): 167.9, 163.6, 146.8, 138.7, 135.6, 134.1, 133.0, 130.6, 129.1, 126.2, 116.9, 111.0, 94.3 (d, *J* = 173 Hz), 65.1, 57.2 (d, *J* = 22 Hz), 49.2, 43.5, 38.2, 33.6, 32.6. Formula: $C_{20}H_{22}Cl_2FN_3O_2$; MS (ESI^+): *m/z* 426 [$M+H^+$].

(3-Chloro-4-fluorophenyl)(4-fluoro-4-(((2-(pyridin-3-yloxy)ethyl)amino)methyl)piperidin-1-yl)methanone (20)

The title compound was prepared using 2-(1-(3-chloro-4-fluorobenzoyl)-4-fluoropiperidin-4-yl)-2-hydroxyacetonitrile (**8**) (0.150 g, 0.48 mmol), 2-(pyridin-3-yloxy)ethanamine (0.105 g, 0.76 mmol), DABCO (0.669 g, 5.97 mmol), sodium cyanoborohydride (0.234 g, 3.73 mmol), molecular sieves (1.043 g) and iron sulfate heptahydrate (0.146 g, 0.53 mmol) in methanol (5 mL). Purification: EtOAc/methanol (9.5/0.5, v/v). Yield: 55%; orange crystallizing oil. ^{1}H NMR (300 MHz, $CDCl_3$, δ): 8.32 (td, *J* = 1.0, 1.7 Hz, 1H), 8.25–8.21 (m, 1H), 7.48 (dd, *J* = 2.1, 6.9 Hz, 1H), 7.33–7.26 (m, 1H), 7.23–7.13 (m, 3H), 4.52 (br s, 1H), 4.11 (t, *J* = 5.1 Hz, 2H), 3.61 (br s, 1H), 3.18 (d, *J* = 5.1 Hz, 2H), 3.05 (t, *J* = 5.1 Hz, 2H), 2.90–2.79 (m, 2H), 2.08–1.95 (m, 2H), 1.79 (br s, 3H). ^{13}C NMR (75 MHz, $CDCl_3$, δ): 168.1, 158.8 (d, *J* = 254 Hz), 154.9, 142.3, 137.9, 132.9 (d, *J* = 4.4 Hz), 129.7, 127.1 (d, *J* = 7.7 Hz), 123.8, 121.5 (d, *J* = 18.2 Hz), 121.1, 116.8 (d, *J* =

21 Hz), 94.3 (d, *J* = 172 Hz), 67.8, 57.3 (d, *J* = 22 Hz), 49.1, 43.6, 38.3, 33.5, 32.8. Formula: $C_{20}H_{22}ClF_2N_3O_2$; MS (ESI^+): *m/z* 410 [$M+H^+$].

(3-Chloro-4-fluorophenyl)(4-fluoro-4-(((2-(pyridin-4-yloxy)ethyl)amino)methyl)piperidin-1-yl)methanone (21)

The title compound was prepared using 2-(1-(3-chloro-4-fluorobenzoyl)-4-fluoropiperidin-4-yl)-2-hydroxyacetonitrile (**8**) (0.300 g, 0.96 mmol), 2-(pyridin-4-yloxy)ethanamine (0.185 g, 1.34 mmol), DABCO (1.34 g, 12.00 mmol), sodium cyanoborohydride (0.467 g, 7.45 mmol), molecular sieves (2.080 g) and iron sulfate heptahydrate (0.292 g, 1.05 mmol) in methanol (9.5 mL). Purification: EtOAc/methanol (9.5/0.5, v/v). Yield: 31%; orange oil. ^1H NMR (300 MHz, $CDCl_3$, δ): 8.19–8.13 (m, 2H), 7.47 (dd, *J* = 2.1, 6.9 Hz, 1H), 7.32–7.27 (m, 1H), 7.21–7.13 (m, 1H), 6.59–6.54 (m, 2H), 4.56 (s, 1H), 3.82 (t, *J* = 5.9 Hz, 2H), 3.68 (d, *J* = 18.7 Hz, 2H), 3.33 (br s, 1H), 3.00 (m, 4H), 2.08 (br s, 2H), 1.90 (br s, 3H). ^{13}C NMR (75 MHz, $CDCl_3$, δ): 168.2, 158.9 (d, *J* = 252 Hz), 154.2, 148.0 (2C), 132.5 (d, *J* = 4.7 Hz), 129.8, 127.2 (d, *J* = 6.9 Hz), 121.6 (d, *J* = 17.5 Hz), 116.9 (d, *J* = 22 Hz), 107.5 (2C), 95.8 (d, *J* = 175 Hz), 58.5, 57.7 (d, *J* = 22 Hz), 52.9, 43.0, 37.8, 33.8, 32.5. Formula: $C_{20}H_{22}ClF_2N_3O_2$; MS (ESI^+): *m/z* 410 [$M+H^+$].

(3-Chloro-4-fluorophenyl)(4-fluoro-4-(((2-(pyrazin-2-yloxy)ethyl)amino)methyl)piperidin-1-yl)methanone (22)

The title compound was prepared using 2-(1-(3-chloro-4-fluorobenzoyl)-4-fluoropiperidin-4-yl)-2-hydroxyacetonitrile (**8**) (0.150 g, 0.48 mmol), 2-(pyrazin-2-yloxy)ethanamine (0.106 g, 0.76 mmol), DABCO (0.669 g, 5.97 mmol), sodium cyanoborohydride (0.234 g, 3.73 mmol), molecular sieves (1.043 g) and iron sulfate heptahydrate (0.146 g, 0.53 mmol) in methanol (5 mL). Purification: EtOAc/methanol (9.8/0.2, v/v). Yield: 40%; yellow crystalizing oil. ^1H NMR (300 MHz, $CDCl_3$, δ): 8.22 (d, *J* = 1.3 Hz, 1H), 8.11 (d, *J* = 2.8 Hz, 1H), 8.06 (dd, *J* = 1.4, 2.7 Hz, 1H),

7.47 (dd, *J* = 2.1, 6.9 Hz, 1H), 7.32–7.26 (m, 1H), 7.21–7.12 (m, 1H), 4.63–4.36 (m, 3H), 3.59 (br s, 1H), 3.27 (br s, 2H), 3.04 (t, *J* = 5.3 Hz, 2H), 2.90–2.77 (m, 2H), 2.00 (br s, 2H), 1.64 (br s, 3H). ^{13}C NMR (75 MHz, $CDCl_3$, δ): 168.1, 160.1, 158.8 (d, *J* = 254 Hz), 140.5, 136.7, 135.9, 132.9 (d, *J* = 4.4 Hz), 129.7, 127.1 (d, *J* = 7.7 Hz), 121.5 (d, *J* = 18.2 Hz), 116.8 (d, *J* = 22 Hz), 94.4 (d, *J* = 172 Hz), 65.7, 57.3 (d, *J* = 22 Hz), 48.9, 43.7, 38.3, 33.6, 33.0. Formula: $C_{19}H_{21}ClF_2N_4O_2$; MS (ESI^+): *m/z* 411 [$M+H^+$].

(3-Chloro-4-fluorophenyl)(4-fluoro-4-(((2-(pyrimidin-2-yloxy)ethyl)amino)methyl)piperidin-1-yl)methanone (23)

The title compound was prepared using 2-(1-(3-chloro-4-fluorobenzoyl)-4-fluoropiperidin-4-yl)-2-hydroxyacetonitrile (**8**) (0.500 g, 1.59 mmol), 2-(pyrimidin-2-yloxy)ethanamine (0.537 g, 2.53 mmol), DABCO (1.160 g, 10.36 mmol), sodium cyanoborohydride (0.595 g, 9.46 mmol), molecular sieves (1.140 g) and iron sulfate heptahydrate (0.486 g, 1.75 mmol) in methanol (17 mL). Purification: EtOAc/methanol (9.5/0.5, v/v). Yield: 47%; orange oil. ^{1}H NMR (300 MHz, $CDCl_3$, δ): 8.52–8.51 (m, 2H), 7.49–7.47 (m, 1H), 7.29–7.28 (m, 1H), 7.20–7.16 (m, 1H), 6.97–6.94 (m, 1H), 4.51 (br s, 1H), 4.48–4.45 (t, *J* = 5.0 Hz, 2H), 3.73–3.15 (m, 3H), 3.08–3.05 (t, *J* = 5.3 Hz, 2H), 2.85 (m, 2H), 2.01 (br s 2H), 1.77–1.50 (m, 3H). ^{13}C NMR (75 MHz, $CDCl_3$, δ): 168.0, 165.1, 159.3 (2C), 158.8 (d, *J* = 252 Hz), 132.9 (d, *J* = 3.5 Hz), 129.7, 127.1 (d, *J* = 6.9 Hz), 121.5 (d, *J* = 17.3 Hz), 116.8 (d, *J* = 22 Hz), 115.2, 94.2 (d, *J* = 172 Hz), 66.9, 57.2 (d, *J* = 22 Hz), 48.9, 43.6, 38.2, 33.4, 32.7. Formula: $C_{19}H_{21}ClF_2N_4O_2$; MS (ESI^+): *m/z* 411 [$M+H^+$].

(3-Chloro-4-fluorophenyl)(4-fluoro-4-(((2-(pyrimidin-5-yloxy)ethyl)amino)methyl)piperidin-1-yl)methanone (24)

The title compound was prepared using 2-(1-(3-chloro-4-fluorobenzoyl)-4-fluoropiperidin-4-yl)-2-hydroxyacetonitrile (**8**) (0.115 g, 0.37 mmol), 2-(pyrimidin-5-yloxy)ethanamine

dihydrochloride (0.090 g, 0.51 mmol), DABCO (0.514 g, 4.78 mmol), sodium cyanoborohydride (0.179 g, 2.86 mmol), molecular sieves (0.900 g) and iron sulfate heptahydrate (0.112 g, 0.40 mmol) in methanol (4 mL). Purification: EtOAc/methanol (8/2, v/v). Yield: 53%; yellow crystalizing oil. ^{1}H NMR (300 MHz, $CDCl_3$, δ): 8.85 (s, 1H), 8.41 (s, 2H), 7.47 (dd, *J* = 2.1, 6.9 Hz, 1H), 7.32–7.26 (m, 1H), 7.21–7.12 (m, 1H), 4.50 (br s, 1H), 4.16 (t, *J* = 5.0 Hz, 2H), 3.60 (br s, 1H), 3.46–3.12 (m, 2H), 3.07 (t, *J* = 5.0 Hz, 2H), 2.91–2.78 (m, 2H), 2.00 (br s, 2H), 1.79–1.55 (m, 3H). ^{13}C NMR (75 MHz, $CDCl_3$, δ): 168.1, 158.8 (d, *J* = 254 Hz), 152.8, 151.7, 143.6 (2C), 132.8 (d, *J* = 3.9 Hz), 129.7, 127.1 (d, *J* = 7.7 Hz), 121.5 (d, *J* = 17.7 Hz), 116.8 (d, *J* = 22 Hz), 94.3 (d, *J* = 172 Hz), 68.3, 57.3 (d, *J* = 22 Hz), 48.9, 43.6, 38.2, 33.6, 32.8. Formula: $C_{19}H_{21}ClF_2N_4O_2$; MS (ESI^+): *m/z* 411 [$M+H^+$].

(3-Chloro-4-fluorophenyl)(4-fluoro-4-(((2-(pyridazin-4-yloxy)ethyl)amino)methyl)piperidin-1-yl)methanone (25)

The title compound was prepared using 2-(1-(3-chloro-4-fluorobenzoyl)-4-fluoropiperidin-4-yl)-2-hydroxyacetonitrile (**8**) (0.150 g, 0.48 mmol), 2-(pyridazin-4-yloxy)ethanamine hydrochloride (0.134 g, 0.76 mmol), DABCO (0.669 g, 5.97 mmol), sodium cyanoborohydride (0.234 g, 3.73 mmol), molecular sieves (1.043 g) and iron sulfate heptahydrate (0.146 g, 0.53 mmol) in methanol (5 mL). Purification: DCM/methanol (9.5/0.5, v/v). Yield: 66%; beige oil. ^{1}H NMR (300 MHz, $CDCl_3$, δ): 7.88 (d, *J* = 3.1 Hz, 1H), 7.76 (d, *J* = 7.7 Hz, 1H), 7.46 (dd, *J* = 2.1, 6.9 Hz, 1H), 7.31–7.24 (m, 1H), 7.22–7.14 (m, 1H), 6.42 (dd, *J* = 3.2, 7.8 Hz, 1H), 4.48 (br s, 1H), 4.08–4.00 (m, 2H), 3.59 (br s, 1H), 3.42–3.14 (m, 2H), 3.13–3.05 (m, 2H), 2.81–2.67 (m, 2H), 1.94 (br s, 2H), 1.70 (br s, 3H). ^{13}C NMR (75 MHz, $CDCl_3$, δ): 170.8, 168.1, 158.8 (d, *J* = 254 Hz), 150.1, 142.1, 132.7 (d, *J* = 4.4 Hz), 129.7, 127.1 (d, *J* = 7.7 Hz), 121.6 (d, *J* = 17.7 Hz), 116.8 (d, *J* = 22 Hz),

116.6, 94.3 (d, *J* = 172 Hz), 59.5, 57.1 (d, *J* = 22 Hz), 48.9, 43.8, 38.2, 33.5, 32.9. Formula: $C_{19}H_{21}ClF_2N_4O_2$; MS (ESI^+): *m/z* 411 [$M+H^+$].

(3-Chloro-4-fluorophenyl)(4-fluoro-4-(((2-((5-methylpyridin-2-yl)oxy)ethyl)amino)methyl)piperidin-1-yl)methanone (26)

The title compound was prepared using 2-(1-(3-chloro-4-fluorobenzoyl)-4-fluoropiperidin-4-yl)-2-hydroxyacetonitrile (**8**) (0.793 g, 2.52 mmol), 2-[(5-methylpyridin-2-yl)oxy]ethanamine (0.500 g, 2.62 mmol), DABCO (1.69 g, 15.24 mmol), sodium cyanoborohydride (1.230 g, 19.66 mmol), molecular sieves (4.580 g) and iron sulfate heptahydrate (0.771 g, 2.77 mmol) in methanol (25 mL). Purification: *n*-hexane/EtOAc (1/9, v/v) and then EtOAc/methanol (9.5/0.5, v/v). Yield: 47%; white oil. ^1H NMR (300 MHz, $CDCl_3$, δ): 7.94–7.9 3 (m., 1H), 7.49–7.47 (m., 1H), 7.41–7.28 (m., 2H), 7.20–7.16 (m., 1H), 6.67–6.65 (d., 1H), 4.51 (m., 1H), 4.38–4.35 (t., *J* = 5.1 Hz, 2H), 3.64–3.18 (m., 3H), 3.04–3.01 (t., *J* = 5.3 Hz, 2H), 2.87–2.82 (d., *J* = 19.9 Hz, 2H), 2.24 (s., 3H), 2.00 (br s., 2H) 1, 83–1.51 (m., 3H). ^{13}C NMR (75 MHz, $CDCl_3$, δ): 168.1, 161.9, 158.8 (d, *J* = 252 Hz), 146.2, 139.8, 132.9 (d, *J* = 3.5 Hz), 129.7, 127.1 (d, *J* = 8.1 Hz), 125.9, 121.5 (d, *J* = 17.3 Hz), 116.8 (d, *J* = 21 Hz), 94.3 (d, *J* = 172 Hz), 65.0, 57.2 (d, *J* = 22 Hz), 49.3, 43.7, 38.2, 33.7, 32.9, 17.4. Formula: $C_{21}H_{24}ClF_2N_3O_2$; MS (ESI^+): *m/z* 424 [$M+H^+$].

(3-Chloro-4-fluorophenyl)(4-fluoro-4-(((2-((5-methylpyrimidin-2-yl)oxy)ethyl)amino)methyl)piperidin-1-yl)methanone (27)

The title compound was prepared using 2-(1-(3-chloro-4-fluorobenzoyl)-4-fluoropiperidin-4-yl)-2-hydroxyacetonitrile (**8**) (1.170 g, 3.72 mmol), 2-(5-methylpyrimidin-2-yloxy)ethanamine (0.600 g, 3.92 mmol), DABCO (2.500 g, 22.50 mmol), sodium cyanoborohydride (1.820 g, 29.02 mmol), molecular sieves (4.800 g) in methanol (17 mL). Purification: EtOAc/methanol/ (9.5/0.5, v/v). Yield: 34%; white crystallizing oil. ^1H NMR ($CDCl_3$, δ): 8.32 (s, 2H), 7.49–7.47 (m, 1H), 7.32–

7.28 (m, 1H), 7.20–7.16 (m, 1H), 4.54 (br s, 1H), 4.44–4.41 (t, *J* = 5.0 Hz, 2H), 3.60–3.16 (m, 3H), 3.06–3.02 (t, *J* = 5.3 Hz, 2H), 2.86 (m, 2H), 2.25 (s, 3H), 2.04 (br s, 2H) 1.81–1.52 (m, 3H). ^{13}C NMR (75 MHz, $CDCl_3$, δ): 168.1, 163.7, 159.1 (2C), 158.8 (d, *J* = 252 Hz), 132.9 (d, *J* = 4.6 Hz), 129.7, 127.1 (d, *J* = 6.9 Hz), 123.9, 121.5 (d, *J* = 18.4 Hz), 116.8 (d, *J* = 21 Hz), 94.3 (d, *J* = 172 Hz), 66.8, 57.3 (d, *J* = 22 Hz), 49.0, 43.3, 38.1, 33.7, 32.7, 14.6. Formula: $C_{20}H_{23}ClF_2N_4O_2$; MS (ESI^+): *m/z* 425 [$M+H^+$].

Developability studies

The PAINS and Brenk alerts, as well as fraction of sp^3 atoms (Fsp^3) were determined using SwissADME server.[53]

Instant JChem was used for structure database management and prediction of the remaining physicochemical parameters, Instant JChem 15.12.14.0, 2015, ChemAxon (http://www.chemaxon.com).

The SafetyScreen44™ Panel (plus additional antitargets), the Bioavailability Panel, CYP3A4, CYP2D6, P-glycoprotein inhibition and cardiac toxicity (hERG automated patch-clamp method) assays were performed by Eurofins Pharma Discovery Services according to the well-known methods. Further methodological details are available on the company Web site (www.eurofinsdiscoveryservices.com) and the appropriate publications. [45, 60-64, 95, 96]

In vitro studies

The tested compounds were examined for known classes of assay interference compounds. None of the compounds contain substructural features recognized as pan assay interference compounds (PAINS), according to SwissADME tool.[53]

Radioligand Binding Assays for 5-HT_{1A}R, α_1R, D_2R

Preparation of solutions of test and reference compounds

1 mM stock solutions of tested compounds were prepared in DMSO. Serial dilutions of compounds were prepared in 96-well microplate in assay buffers using automated pipetting system epMotion 5070 (Eppendorf). Each compound was tested in 10 concentrations from 1.0E-06 to 1.0E-12 M (final concentration).

Serotonin 5-HT_{1A} Receptor Binding Assay

Radioligand binding was performed using membranes from CHO-K1 cells stably transfected with the human 5-HT_{1A} receptor (PerkinElmer). All assays were carried out in duplicates. 50 µL working solution of the tested compounds, 50 µL [^{3}H]-8-OH-DPAT (final concentration 1 nM) and 150 µL diluted membranes (10 µg protein per well) prepared in assay buffer (50 mM Tris, pH 7.4, 10 mM $MgSO_4$, 0, 5 mM EDTA, 0.1% ascorbic acid) were transferred to polypropylene 96-well microplate using 96-wells pipetting station Rainin Liquidator (MettlerToledo). Serotonin (10 µM) was used to define nonspecific binding. Microplate was covered with a sealing tape, mixed and incubated for 60 minutes at 27 °C. The reaction was terminated by rapid filtration through GF/C filter mate presoaked with 0.3% polyethyleneimine for 30 minutes. Ten rapid washes with 200 µL 50 mM Tris buffer (4 °C, pH 7.4) were performed using automated harvester system

Harvester-96 MACH III FM (Tomtec). The filter mates were dried at 37 °C in forced air fan incubator and then solid scintillator MeltiLex was melted on filter mates at 90 °C for 4 minutes. Radioactivity was counted in MicroBeta2 scintillation counter (PerkinElmer). Data were fitted to a one-site curve-fitting equation with Prism 6 (GraphPad Software) and Ki values were estimated from the Cheng−Prusoff equation.

Adrenergic α_1 Receptor Binding Assay

Radioligand binding was performed using rat cortex. Tissue was homogenized in 20 volumes of ice-cold 50 mM Tris-HCl buffer, pH 7.6 using an Ultra Turrax T25B (IKA) homogenizer. The homogenate was centrifuged at 20, 000 x g for 20 min. The resulting supernatant was decanted and pellet was resuspended in the same buffer and centrifuged again in the same conditions. The final pellet was resuspended in appropriate volume of buffer (10 mg/1ml). All assays were carried out in duplicates. 50 μL working solution of the tested compounds, 50 μL [^{3}H]-prazosin (final concentration 0.2 nM) and 150 μL tissue suspension were transferred to polypropylene 96-well microplate using 96-wells pipetting station Rainin Liquidator (MettlerToledo). Phentolamine (10 μM) was used to define nonspecific binding. Microplate was covered with a sealing tape, mixed and incubated for 30 minutes at 30 °C. The incubation was terminated by rapid filtration over glass fiber filters FilterMate B (PerkinElmer, USA) using 96-well FilterMate harvester (PerkinElmer, USA). Five rapid washes were performed with ice-cold 50 mM Tris-HCl buffer, pH 7.6. The filter mates were dried at 37 °C in forced air fan incubator and then solid scintillator MeltiLex was melted on filter mates at 90 °C for 5 minutes. Radioactivity was counted in MicroBeta2 scintillation counter (PerkinElmer). Data were fitted to a one-site curve-fitting equation with Prism 6 (GraphPad Software) and Ki values were estimated from the Cheng−Prusoff equation.

Dopamine D_2 Receptor Binding Assay

Radioligand binding was performed using membranes from CHO-K1 cells stably transfected with the human D_2 receptor (PerkinElmer). All assays were carried out in duplicates. 50 µL working solution of the tested compounds, 50 µL [^{3}H]-methylspiperone (final concentration 0.4 nM) and 150 µL diluted membranes (3 µg protein per well) prepared in assay buffer (50 mM Tris, pH 7.4, 50 mM HEPES, 50 mM NaCl, 5 mM $MgCl_2$, 0.5 mM EDTA) were transferred to polypropylene 96-well microplate using 96-wells pipetting station Rainin Liquidator (MettlerToledo). Haloperidol (10 µM) was used to define nonspecific binding. Microplate was covered with a sealing tape, mixed and incubated for 60 minutes at 37 °C. The reaction was terminated by rapid filtration through GF/B filter mate presoaked with 0.5% polyethyleneimine for 30 minutes. Ten rapid washes with 200 µL 50 mM Tris buffer (4 °C, pH 7.4) were performed using automated harvester system Harvester-96 MACH III FM (Tomtec). The filter mates were dried at 37 °C in forced air fan incubator and then solid scintillator MeltiLex was melted on filter mates at 90 °C for 5 minutes. Radioactivity was counted in MicroBeta2 scintillation counter (PerkinElmer). Data were fitted to a one-site curve-fitting equation with Prism 6 (GraphPad Software) and Ki values were estimated from the Cheng−Prusoff equation.

5-HT_{1A} saturation binding assay

[^{3}H]-8-OH-DPAT, [Propyl-2,3-ring-1,2,3-3H], spec. act. 135.2 Ci/mmol, 1mCi/mL, PerkinElmer) was used for labeling 5-HT_{1A}Rs. Saturation binding studies were performed using membranes from CHO-K1/U2OS cells stably transfected with the human 5-HT_{1A} receptor (PerkinElmer). All assays were carried out in triplicates. 50 µL of [^{3}H]-8-OH-DPAT solution (10 concentrations ranging from 0.4 to 14 nM), 50 µL Tris–HCl buffer (total binding) or 50 µL of 10 µM serotonin

(nonspecific binding) and 150 µL diluted membranes (20 µg protein per well) prepared in assay buffer (50 mM Tris, pH 7.4, 10 mM $MgSO_4$, 0.5 mM EDTA, 0.1% ascorbic acid) were transferred to polypropylene 96-well microplate using 96-wells pipetting station Rainin Liquidator (MettlerToledo). Microplate was covered with a sealing tape, mixed and incubated for 60 minutes at 27 °C. The reaction was terminated by rapid filtration through GF/B filter mate presoaked with 0.5% polyethyleneimine for 30 minutes. Ten rapid washes with 200 µL 50 mM Tris buffer (4 °C, pH 7.4) were performed using automated harvester system Harvester-96 MACH III FM (Tomtec). The filter mates were dried at 37 °C in forced air fan incubator and then solid scintillator MeltiLex was melted on filter mates at 90 °C for 4 minutes. Radioactivity was counted in MicroBeta2 scintillation counter (PerkinElmer). Data were calculated using Prism 5 (GraphPad Software) and B_{max} and K_D values were estimated from the one-site specific binding saturation curve.

Functional assays for the 5-HT$_{1A}$ receptor

ERK1/2 phosphorylation

Test and reference compounds were dissolved in dimethyl sulfoxide (DMSO) at a concentration of 10 mM. Serial dilutions were prepared in 96-well microplate in HBSS with 0.1% BSA added and 8 concentrations were tested.

The CHO-5HT$_{1A}$ receptor cells were tested for agonist-induced ERK1/2-phosphorylation using the SureFire ERK1/2-Phosphorylation Alpha LISA assay kit according to the manufacturer's instruction (Perkin Elmer). After thawing, cells were cultured in medium (Advanced DMEM/F12 with 1% FBS dialyzed, 400µg/mL G-418, 4 mM L-Glutamine). At the experiment cells were plated at 50, 000 cells/well of 96-well tissue culture plate and grown 7 hours in incubator (5% CO_2, 37 °C), after this time the cells were starving (DMEM/F12 with 0, 1% BSA (immunoglobulin- and protease-free) for 12 hours. The serial dilutions of compounds were added and incubated for 15 minutes in 37 °C. The medium was removed, "lysis buffer" (70 µL) was added and the plate gently agitated on a plate shaker (10 minutes). The plates were freezing in -80 °C. The next day, plate were thawing on plate shaker for 10 minutes and 10 µL were transferred to assay plates (384-OptiPlate, Perkin Elmer) in duplicate and 10 µL of reaction mix AlphaLISA SureFire Ultra assay (Perkin Elmer) were added. The plate were incubated for 2 hours in 22 °C. After incubation, the assay plate were measured in an EnVision multifunction plate reader (Perkin Elmer Life Science). E_{max} values were defined as the response of the ligand expressed as a percentage of the maximal response elicited by serotonin, determined by nonlinear regression using GraphPad Prism 6.0 software. pEC$_{50}$ values correspond to the ligand concentration at which 50% of its own maximal response was measured.

cAMP inhibition

Tested and reference compounds were dissolved in dimethyl sulfoxide (DMSO) to the concentration of 10 mM. Dilutions were prepared in 96-well microplate in assay buffers. For 5-HT_{1A} receptors, adenylyl cyclase activity was determined using cryopreserved CHO-K1 cells with expression of the human serotonin 5-HT_{1A} receptor.

The functional assay was performed with the CHO-K1 cells with expression of the 5-HT_{1A} human serotonin receptor where plasmid containing the coding sequence was transfected in. The cells were cultured under selective conditions (400 μg/mL Geneticin G418) (Perkin Elmer). Thawed cells were resuspended in stimulation buffer (HBSS, 5 mM HEPES, 0.5 IBMX, and 0.1% BSA at pH 7.4) at 2×10^5 cells/mL. The same volume (10 μl) of cell suspension was added to tested compounds with 10 μM forskolin. Samples were loaded onto a white opaque half area 96-well microplate. Cell stimulation was performed for 40 min at room temperature. After incubation, cAMP measurements were performed with homogeneous TR-FRET immunoassay using the LANCE Ultra cAMP kit (PerkinElmer, USA). 10 μL of EucAMP Tracer Working Solution and 10 μL of ULight-anti-cAMP Tracer Working Solution were added, mixed, and incubated for 1 h. The TR-FRET signal was read on an EnVision microplate reader (PerkinElmer, USA). E_{max} values were defined as the response of the ligand expressed as a percentage of the maximal response elicited by serotonin, determined by nonlinear regression using GraphPad Prism 6.0 software. pEC_{50} values correspond to the ligand concentration at which 50% of its own maximal response was measured.

β-arrestin recruitment

Test and reference compounds were dissolved in dimethyl sulfoxide (DMSO) at a concentration of 10 mM. Serial dilutions were prepared in 96-well microplate in DMEM medium with 10% FBS added and 8 concentrations were tested.

The HTR1A-bla U2OS receptor cells contain the human Serotonin Type 1A receptor linked to a TEV protease site and a Gal4-VP16 transcription factor, were tested for agonist-induced using the Tango LiveBLAzer assay kit according to the manufacturer's instruction (Life Technologies). After thawing, cells were cultured in medium (McCoy's 5A with 10% FBS dialyzed, 0.1 mM NEAA, 25 mM HEPES, 1mM Sodium Pyruvate, 100 μg/mL G-418, 100 U/mL Penicillin/Streptomycin Antibiotic, 200 μg/mL Zeocin, 50 μg/mL Hygromycin). At the experiment cells were plated at 10, 000 cells/well of 384-well black, clear bottom, tissue culture plate and grown 12 hours in incubator (5% CO_2, 37 °C) in DMEM medium with 10% FBS added. The serial dilutions of compounds were added and incubated for 5 hours (5% CO_2, 37 °C). After this time, 8 μL of reaction mix were added. The plate were incubated for 2 hours in 22 °C. After incubation, the assay plate were measured in an FLUOstar Optima a multifunction plate reader (Perkin Elmer Life Science). E_{max} values were defined as the response of the ligand expressed as a percentage of the maximal response elicited by serotonin, determined by nonlinear regression using GraphPad Prism 6.0 software. pEC_{50} values correspond to the ligand concentration at which 50% of its own maximal response was measured.

Calcium mobilization assay

CHO-K1 cells with stable expression of human $5HT_{1A}$ receptor were cultured according to the manufacturer's instruction (Perkin Elmer) in standard medium (Advanced DMEM/F12 with 1%

FBS dialyzed, 400μg/mL G-418, 4 mM L-Glutamine). At the experiment cells were plated at 60,000 cells/well of 96-well tissue culture plate and grown 12 hours and incubated (5% CO_2, 37 °C). Cells after grown in 96-well plates, were washed two times with HBSS assay buffer (137 mM NaCl, 5.4 mM KCl, 0.25 mM Na_2HPO_4, 0.44 mM KH_2PO_4, 1.3 mM $CaCl_2$, 1.0 mM $MgSO_4$, 1.0 mM $MgCl_2$, 10 mM glucose, 10 mM HEPES, 2 mM Probenecid, 0.1% BSA with pH adjusted to 7.4 using 1.0 M HCl). Next, the 3 μM Fluo-4AM in loading buffer containig 0,04% w/v Pluronic F-127 at 100 μL was added to each well and the plate was incubated at 37 °C for 1 h. Cells were washed two times with the assay buffer and 100 μl of the assay buffer was dispensed to each well. Fluorescence readings (ex 485 nm, 520 nm) were performed with the Omega POLARStar microplate reader (BMG Labtech, Germany). After recording the baseline, 50 μL of a 3-fold dilution of the tested compounds was added to each well and kinetic was measured for 180 seconds with 2-second intervals. E_{max} values were defined as the response of the ligand expressed as a percentage of the maximal response elicited by serotonin, determined by nonlinear regression using GraphPad Prism 6.0 software. pEC_{50} values correspond to the ligand concentration at which 50% of its own maximal response was measured.[97]

In vivo and *ex vivo* pharmacodynamic studies

Animals

The experiments were performed on male Wistar rats (170–200 g) obtained from an accredited animal facility at the Jagiellonian University Medical College, Krakow, Poland. The animals were housed in group of four in controlled environment (ambient temperature 21 ± 2 °C; relative humidity 50–60%; 12 h light/dark cycles (lights on at 8:00). Standard laboratory food (LSM-B) and filtered water were freely available. Animals were housed for a period of 6 days in polycarbonate Makrolon type 3 cages (dimensions 26.5×15×42 cm, ‘open top’) without

enrichment environment (only wooden shavings litter). Each animal was assigned randomly to treatment groups and only used once (no repeated use of animals). All the experiments were performed by two observers unaware of the treatment applied between 9:00 and 14:00 on separate groups of animals. All procedures involving animals and their care were conducted in accordance with current European Community and Polish legislation on animal experimentation. Additionally, efforts were made to minimize animal suffering and to use only the number of animals necessary to produce reliable scientific data. All experimental procedures involving animals were conducted in accordance with European Union (Directive 2010/63/EU) and Polish legislation acts concerning animal experimentation and approved by the II Local Ethics Committee for Experiments on Animals in Cracow, Poland (approval number: 108/2016). All efforts were made to minimize suffering and to reduce the number of animals used in the experiments.

Drugs

All drugs were dissolved in distilled water immediately before administration in a volume of 2 mL/kg. The examined compound was administered orally 60 and 15 min before tests. In antagonism experiments, WAY100635 (Tocris, UK) was administered subcutaneously (s.c.) 75 min. and 30 min before testing, respectively. Control animals received vehicle (distilled water) according to the same schedule.

Forced swim test (FST)

The experiment was carried out according to method of Porsolt et.al.[85] On the first day of an experiment, the animals were individually gently placed in Plexiglas cylinders (40 cm high, 18 cm in diameter) containing 17 cm of water maintained at 23–25 °C for 15 min. On removal from water, the rats were placed for 30 min in a Plexiglas box under a 60 W bulb to dry. On the following day (24 h later), the rats were re-placed in the cylinder after administration of test compounds and

the total duration of immobility was recorded during the 5-min test period. Immobility was considered to occur when no additional activity was observed other than that necessary to keep the rat's head above the water.[98] Fresh water was used for each animal.

Flat body posture

Observations were made from 55 to 65 min after p.o. treatment according to the method described by Kleven et al.[99] Animals were observed individually during each 10 min period; every 15 s with a period of 10 s of observation per animal. Flat body posture (FBP) was scored present (1) if it occurred during the entire observation period; otherwise, the score was 0.

Spontaneous locomotor activity

The experiment was performed using Motor Monitor System (Campden Instruments, Ltd., UK) consisted of two SmartFrame Open Field stations (40 x 40 x 38 cm) with 16 x 16 beams, located in sound attenuating chambers and connected to PC software by control chassis. Individual vehicle- or drug-injected animals were gently placed in the center of the station. An automated Motor Monitor System recorded ambulation (in X and Y axis), the number of rearing episodes, and total distance covered by a rat for 5 min.

***Ex vivo* studies of the pERK1/2 level in prefrontal cortex**

Experimental design

In the time-course study, compound **17,** or vehicle, was administered orally at the dose of 2.5 mg/kg and the animals were decapitated at the following time points after administration: 5, 15, 30, and 60 minutes (n = 6–8 rats per each time point). In the dose-effect study, compound **17** was administered p.o. at different doses (0.04, 0.16, 0.63 and 2.5 mg/kg; n = 6–8 rats per each dose), then rats were decapitated 15 minutes after administration.

pERK1/2 and total ERK1/2 measurement in brain tissue

Brains of the rats were removed immediately after decapitation, cooled on dry ice and prefrontal cortex was isolated. After tissue dissection and storage in -80 °C, the tissue was thawed on dry ice and homogenized with a TissueRuptor homogenizer in 0.35 mL of buffer lysis (Perkin Elmer) with protease inhibitor cocktail added. After homogenization the tissue were immediately frozen in liquid nitrogen, defrosted on ice and homogenized again. The tissue lysates were centrifuged at 13 000 rpm for 20 min at 4 ºC, and the pellets were discarded. The total protein concentrations in the lysates were determined using a BCA (bicinchoninic acid) assay (Sigma Aldrich) with bovine serum albumin as the standard. Subsequently, the supernatant fluid was transferred to another tube and stored at -80 °C until phosho-ERK1/2 and total-ERK1/2 were tested. The next day probes were thawing for 20 minutes on ice and 10 µL of homogenates containing 10 µg proteins were transferred to assay plates (384-OptiPlate, Perkin Elmer) in duplicate. The 10 µL of reaction mix AlphaLISA SureFire Ultra assay (Perkin Elmer) were added. The plates were incubated for 2 hours in 22 °C. After incubation, the assay plates were measured in an EnVision multifunction plate reader (Perkin Elmer Life Science). All samples were tested in duplicates. The results were calculated as a percent of control after dividing the phosho-ERK1/2 by total-ERK1/2.

Statistical analysis

The data of behavioral studies were evaluated by an analysis of variance: one-way ANOVA (when one drug was given) or two-way ANOVA (when two drugs were used) followed by Bonferroni's post hoc test (statistical significance set at $p<0.05$). For the time-course and dose-effect studies, the value of pERK1/2 was divided by the corresponding value of total-ERK1/2 for each sample, then the ratios were used for statistical analysis of variance (ANOVA) followed by Bonferroni's post hoc ($p<0.05$ was considered statistically significant). The data were expressed as the mean ±

SEM (2 measures for each rat per group). The mean value of the control group was set at 100% (control value) and all data were expressed as a percentage relative to the control value.

In vivo pharmacokinetic studies

Analytical method

Extraction procedure

Serum samples (100 μl) containing compound **17** were spiked with 10 μL of internal standard solution (compound **16**). The samples were alkalized with 100 μL of 1 M sodium hydroxide solution, vortex-mixed and extracted with 1 mL of ethyl acetate/hexane (30/70, v/v) mixture on a shaker (VXR Vibrax, IKA, Germany) for 15 min. After centrifugation (TDx Centrifuge, Abbott Laboratories, USA), the organic layers were transferred into new tubes containing 100 μL of a methanol and 0.1 M sulfuric acid (10/90, v/v) mixture. Then the samples were shaken and centrifuged again. Finally, 10-70 μL of each acidic layer were injected into the HPLC system.

Equipment and chromatographic conditions

The HPLC system consisted of a P100 pump (Thermo Separation Products, San Jose, CA, USA), an L-2200 autosampler, and an L-2420 UV/VIS detector (Merck-Hitachi). EZChrome Elite v. 3.2 software (Merck Hitachi) was used for data acquisition. The pump was used under isocratic conditions on a manual mode. The chromatographic separation of compound **17** and the internal standard was achieved at room temperature (22 ± 1 ^{o}C) on the Supelcosil^{TM} LC-PCN column 250×4.6 mm (Sigma-Aldrich, Germany) with 5 μm particles, protected with the Supelcosil$^{™}$ LC-PCN guard column (Sigma-Aldrich, Germany). The mobile phase consisted of 25 mM potassium dihydrogen phosphate buffer, pH 4.6:methanol: acetonitrile (51/40/9, v/v/v). The flow rate was 1.0 mL/min and the detection wavelength was set at 205 nm.

Validation of the assay was performed according to the FDA guideline (Bioanalytical method validation).[100] This included selectivity, linearity, accuracy and precision, limit of detection (LOD) and limit of quantitation (LOQ), recovery, and stability.

Pharmacokinetic study

In order to assess pharmacokinetics and brain penetration of compound **17**, blood samples and brains were harvested following each pharmacological experiment up to 60 min after dosing. The rats were sacrificed by decapitation.

Blood was allowed to clot for 15 min at room temperature, and then centrifuged (12000 rpm for 5 min). The obtained serum and brains were stored frozen at –80 ^{o}C until analysis.

Pharmacokinetic and PK/PD analysis

Serum concentration versus time data were analyzed by a non-compartmental approach. The maximum concentration (Cmax) and the time to reach peak concentration (Tmax) following oral dosing were obtained directly from the concentration versus time data. The terminal elimination rate constant (λz) was assessed by linear regression. Terminal half-life ($t0.5\lambda z$) was calculated as $\ln 2/\lambda z$. Area under the concentration-time curve from the time of dosing to infinity ($AUC0\text{-}\infty$) was calculated by the linear trapezoidal rule. The extrapolated terminal area was defined as $Cn/\lambda z$, where Cn is the last data point. Apparent volume of distribution (Vz/F) during terminal phase was estimated as $Dosepo/(AUCinf\cdot\lambda z)$, where F is the fraction of dose absorbed. Data were presented as mean±SEM. The simple Emax or sigmoid inhibitory Emax models were fitted to effect-concentration data using Phoenix WinNonlin v. 7.0 (Pharsight Corporation, a Certara Company, Princeton, NJ, USA).

ASSOCIATED CONTENT

Supporting information

Molecular Formula Strings (MFS), The tables of functional activity data with SEM values, radioligand binding assay results and methodology for 5-HT_{2A}, M_1 and H_1 receptors, dose-response curves for functional activity and detailed data of the effects of compound **17** in the FST test were included. This material is available free of charge on the ACS Publications website at http://pubs.acs.org.

AUTHOR INFORMATION

Corresponding Author

Phone: (48)126205460 Fax: (48)126205458.

E-mail: marcin.kolaczkowski@uj.edu.pl

Author Contributions

All authors have contributed and have given approval to the final version of the manuscript.

Notes

The authors declare the following competing financial interest(s): M.A.V. and A.N.-T. are employees and shareholders of Neurolixis Inc.

ACKNOWLEDGMENT

This study was financially supported by The National Science Centre (NCN) Grant No. 2015/19/B/NZ7/03543.

ABBREVIATIONS

ADME, absorption distribution metabolism and excretion; BBB, blood brain barrier; cAMP – cyclic adenosine monophosphate; CNS MPO, Central Nervous System Multiparameter Optimization; ERK1/2, extracellular signal–regulated kinase 1/2; F13640 (befiradol), {[1-(3-chloro-4-fluorobenzoyl)-4-fluoropiperidin-4-yl]methyl}[(5-methylpyridin-2-yl)methyl]amine; F13714, 6-[({[1-(3-chloro-4-fluorobenzoyl)-4-fluoropiperidin-4-yl]methyl}amino)methyl]-*N*,3-dimethylpyridin-2-amine; **1** (F15599), {[1-(3-chloro-4-fluorobenzoyl)-4-fluoropiperidin-4-yl]methyl}[(5-methylpyrimidin-2-yl)methyl]amine; FBP, flat body; FPT, forepaw treading; Fsp^3, ratio of sp^3 carbons to the total number of carbons within the molecule; FST, forced swimming test (Porsolt test); IFD, induced fit docking, LE, ligand efficiency; LELP, ligand efficiency-dependent lipophilicity; LLE, lipophilic ligand efficiency; LLR, lower lip retraction; mPCT, medial prefrontal cortex; PAINS, Pan-Assay INterference compoundS; PBS, phosphate-buffered saline; PFC, prefrontal cortex; Ro5, Lipinski's rule of five; SGF, simulated gastric fluid; SIF, simulated intestinal fluid; TLC, thin layer chromatography WAY-100635, *N*-[2-[4-(2-methoxyphenyl)piperazin-1-yl]ethyl]-*N*-pyridin-2-ylcyclohexanecarboxamide;

REFERENCES

(1) Penn, E.; Tracy, D. K. The Drugs Don't Work? Antidepressants and the Current and Future Pharmacological Management of Depression. *Ther. Adv. Psychopharmacol.* **2012**, *2* (5), 179–188.

(2) Montgomery, S. A. Why Do We Need New and Better Antidepressants? *Int. Clin. Psychopharmacol.* **2006**, *21 Suppl 1*, S1–S10.

(3) Baghai, T. C.; Blier, P.; Baldwin, D. S.; Bauer, M.; Goodwin, G. M.; Fountoulakis, K. N.; Kasper, S.; Leonard, B. E.; Malt, U. F.; Stein, D.; Versiani, M.; Möller, H. J. General and Comparative Efficacy and Effectiveness of Antidepressants in the Acute Treatment of Depressive Disorders: A Report by the WPA Section of Pharmacopsychiatry. *Eur. Arch. Psychiatry Clin. Neurosci.* **2011**, *261* (3), 207–245.

(4) Tylee, A.; Walters, P. Onset of Action of Antidepressants. *BMJ* **2007**, *334* (7600), 911–912.

(5) Courtet, P.; Lopez-Castroman, J. Antidepressants and Suicide Risk in Depression. *World Psychiatry* **2017**, *16* (3), 317–318.

(6) Lener, M. S.; Kadriu, B.; Zarate, C. A. Ketamine and Beyond: Investigations into the Potential of Glutamatergic Agents to Treat Depression. *Drugs* **2017**, *77* (4), 381–401.

(7) Rakesh, G.; Pae, C.-U.; Masand, P. S. Beyond Serotonin: Newer Antidepressants in the Future. *Expert Rev. Neurother.* **2017**, *17* (8), 777–790.

(8) Serafini, G.; Howland, R. H.; Rovedi, F.; Girardi, P.; Amore, M. The Role of Ketamine in Treatment-Resistant Depression: A Systematic Review. *Curr. Neuropharmacol.* **2014**, *12* (5), 444–461.

(9) Fernandes, A.; Li, Y.-W. Focused Microwave Irradiation-Assisted Immunohistochemistry to Study Effects of Ketamine on Phospho-ERK Expression in the Mouse Brain. *Brain Res.* **2017**, *1670*, 86–95.

(10) Lepack, A. E.; Bang, E.; Lee, B.; Dwyer, J. M.; Duman, R. S. Fast-Acting Antidepressants Rapidly Stimulate ERK Signaling and BDNF Release in Primary Neuronal Cultures. *Neuropharmacology* **2016**, *111*, 242–252.

(11) Réus, G. Z.; Vieira, F. G.; Abelaira, H. M.; Michels, M.; Tomaz, D. B.; dos Santos, M. A. B.; Carlessi, A. S.; Neotti, M. V.; Matias, B. I.; Luz, J. R.; Dal-Pizzol, F.; Quevedo, J. MAPK Signaling Correlates with the Antidepressant Effects of Ketamine. *J. Psychiatr. Res.* **2014**, *55*, 15–21.

(12) Pochwat, B.; Rafało-Ulińska, A.; Domin, H.; Misztak, P.; Nowak, G.; Szewczyk, B. Involvement of Extracellular Signal-Regulated Kinase (ERK) in the Short and Long-Lasting Antidepressant-like Activity of NMDA Receptor Antagonists (Zinc and Ro 25-6981) in the Forced Swim Test in Rats. *Neuropharmacology* **2017**, *125*, 333–342.

(13) Niciu, M. J.; Shovestul, B. J.; Jaso, B. A.; Farmer, C.; Luckenbaugh, D. A.; Brutsche, N. E.; Park, L. T.; Ballard, E. D.; Zarate, C. A. Features of Dissociation Differentially Predict Antidepressant Response to Ketamine in Treatment-Resistant Depression. *J. Affect. Disord.* **2018**, *232*, 310–315.

(14) Bartoli, F.; Clerici, M.; Carrà, G. Antidepressant Response and Dissociative Effects After Ketamine Treatment: Two Sides of the Same Coin? *J. Clin. Psychiatry* **2017**, *78* (9), e1318.

(15) Huang, Y.-C.; Jeng, C.-M.; Cheng, T.-C. Ketamine-Associated Ulcerative Cystitis. *Tzu Chi Med. J.* **2008**, *20* (2), 144–146.

(16) Riva-Posse, P.; Reiff, C. M.; Edwards, J. A.; Job, G. P.; Galendez, G. C.; Garlow, S. J.; Saah, T. C.; Dunlop, B. W.; McDonald, W. M. Blood Pressure Safety of Subanesthetic Ketamine for Depression: A Report on 684 Infusions. *J. Affect. Disord.* **2018**, *236*, 291–297.

(17) Mason, K.; Cottrell, A. M.; Corrigan, A. G.; Gillatt, D. A.; Mitchelmore, A. E. Ketamine-Associated Lower Urinary Tract Destruction: A New Radiological Challenge. *Clin. Radiol.* **2010**, *65* (10), 795–800.

(18) Gigliucci, V.; O'Dowd, G.; Casey, S.; Egan, D.; Gibney, S.; Harkin, A. Ketamine Elicits Sustained Antidepressant-like Activity via a Serotonin-Dependent Mechanism. *Psychopharmacology (Berl.)* **2013**, *228* (1), 157–166.

(19) Fukumoto, K.; Iijima, M.; Funakoshi, T.; Chaki, S. Role of 5-HT1A Receptor Stimulation in the Medial Prefrontal Cortex in the Sustained Antidepressant Effects of Ketamine. *Int. J. Neuropsychopharmacol.* **2018**, *21* (4), 371–381.

(20) Fukumoto, K.; Iijima, M.; Chaki, S. Serotonin-1A Receptor Stimulation Mediates Effects of a Metabotropic Glutamate 2/3 Receptor Antagonist, 2S-2-Amino-2-(1S,2S-2-Carboxycycloprop-1-Yl)-3-(Xanth-9-Yl)Propanoic Acid (LY341495), and an N-Methyl-D-Aspartate Receptor Antagonist, Ketamine, in the Novelty-Suppressed Feeding Test. *Psychopharmacology (Berl.)* **2014**, *231* (11), 2291–2298.

(21) Albert, P. R.; Vahid-Ansari, F.; Luckhart, C. Serotonin-Prefrontal Cortical Circuitry in Anxiety and Depression Phenotypes: Pivotal Role of Pre- and Post-Synaptic 5-HT1A Receptor Expression. *Front. Behav. Neurosci.* **2014**, *8*, 199.

(22) Kimbrell, T. A.; Ketter, T. A.; George, M. S.; Little, J. T.; Benson, B. E.; Willis, M. W.; Herscovitch, P.; Post, R. M. Regional Cerebral Glucose Utilization in Patients with a Range of Severities of Unipolar Depression. *Biol. Psychiatry* **2002**, *51* (3), 237–252.

(23) Cervo, L.; Samanin, R. Potential Antidepressant Properties of 8-Hydroxy-2-(Di-n-Propylamino)Tetralin, a Selective Serotonin1A Receptor Agonist. *Eur. J. Pharmacol.* **1987**, *144* (2), 223–229.

(24) Luscombe, G. P.; Martin, K. F.; Hutchins, L. J.; Gosden, J.; Heal, D. J. Mediation of the Antidepressant-like Effect of 8-OH-DPAT in Mice by Postsynaptic 5-HT1A Receptors. *Br. J. Pharmacol.* **1993**, *108* (3), 669–677.

(25) Miyata, S.; Hirano, S.; Kamei, J. Diabetes Attenuates the Antidepressant-like Effect Mediated by the Activation of 5-HT1A Receptor in the Mouse Tail Suspension Test. *Neuropsychopharmacol. Off. Publ. Am. Coll. Neuropsychopharmacol.* **2004**, *29* (3), 461–469.

(26) Prinsze, C.; Stevens, G. Flesinoxan in the Treatment of Major Depressive Disorder: A Fixed Dose, Placebo-Controlled Trial. *Eur. Neuropsychopharmacol.* **1996**, *6*, S4-73.

(27) Newman-Tancredi, A.; Martel, J.-C.; Assié, M.-B.; Buritova, J.; Lauressergues, E.; Cosi, C.; Heusler, P.; Bruins Slot, L.; Colpaert, F. C.; Vacher, B.; Cussac, D. Signal Transduction and Functional Selectivity of F15599, a Preferential Post-Synaptic 5-HT1A Receptor Agonist. *Br. J. Pharmacol.* **2009**, *156* (2), 338–353.

(28) Maurel, J. L.; Autin, J.-M.; Funes, P.; Newman-Tancredi, A.; Colpaert, F.; Vacher, B. High-Efficacy 5-HT1A Agonists for Antidepressant Treatment: A Renewed Opportunity. *J. Med. Chem.* **2007**, *50* (20), 5024–5033.

(29) Becker, G.; Bolbos, R.; Costes, N.; Redouté, J.; Newman-Tancredi, A.; Zimmer, L. Selective Serotonin 5-HT1A Receptor Biased Agonists Elicitdistinct Brain Activation Patterns: A PharmacoMRI Study. *Sci. Rep.* **2016**, *6*, 26633.

(30) Lladó-Pelfort, L.; Assié, M.-B.; Newman-Tancredi, A.; Artigas, F.; Celada, P. Preferential in Vivo Action of F15599, a Novel 5-HT(1A) Receptor Agonist, at Postsynaptic 5-HT(1A) Receptors. *Br. J. Pharmacol.* **2010**, *160* (8), 1929–1940.

(31) Assié, M.-B.; Bardin, L.; Auclair, A. L.; Carilla-Durand, E.; Depoortère, R.; Koek, W.; Kleven, M. S.; Colpaert, F.; Vacher, B.; Newman-Tancredi, A. F15599, a Highly Selective Post-Synaptic 5-HT(1A) Receptor Agonist: In-Vivo Profile in Behavioural Models of Antidepressant and Serotonergic Activity. *Int. J. Neuropsychopharmacol.* **2010**, *13* (10), 1285–1298.

(32) Jastrzębska-Więsek, M.; Partyka, A.; Rychtyk, J.; Śniecikowska, J.; Kołaczkowski, M.; Wesołowska, A.; Varney, M. A.; Newman-Tancredi, A. Activity of Serotonin 5-HT1AReceptor Biased Agonists in Rat: Anxiolytic and Antidepressant-like Properties. *ACS Chem. Neurosci.* **2018**. *9* (5), 1040–1050.

(33) van Goethem, N. P.; Schreiber, R.; Newman-Tancredi, A.; Varney, M.; Prickaerts, J. Divergent Effects of the "biased" 5-HT1 A Receptor Agonists F15599 and F13714 in a Novel Object Pattern Separation Task. *Br. J. Pharmacol.* **2015**, *172* (10), 2532–2543.

(34) Newman-Tancredi, A. Biased Agonism at Serotonin 5HT1A Receptors: Preferential Postsynaptic Activity for Improved Therapy of CNS Disorders. *Neuropsychiatry* **2011**, *1* (2).

(35) Depoortère, R.; Auclair, A. L.; Bardin, L.; Colpaert, F. C.; Vacher, B.; Newman-Tancredi, A. F15599, a Preferential Post-Synaptic 5-HT1A Receptor Agonist: Activity in Models of

Cognition in Comparison with Reference 5-HT1A Receptor Agonists. *Eur. Neuropsychopharmacol. J. Eur. Coll. Neuropsychopharmacol.* **2010**, *20* (9), 641–654.

(36) Yokoyama, C.; Mawatari, A.; Kawasaki, A.; Takeda, C.; Onoe, K.; Doi, H.; Newman-Tancredi, A.; Zimmer, L.; Onoe, H. Marmoset Serotonin 5-HT1A Receptor Mapping with a Biased Agonist PET Probe 18F-F13714: Comparison with an Antagonist Tracer 18F-MPPF in Awake and Anesthetized States. *Int. J. Neuropsychopharmacol.* **2016**, *19* (12).

(37) de Boer, S. F.; Newman-Tancredi, A. Anti-Aggressive Effects of the Selective High-Efficacy "biased" 5-HT_1A Receptor Agonists F15599 and F13714 in Male WTG Rats. *Psychopharmacology (Berl.)* **2016**, *233* (6), 937–947.

(38) Bucki, A.; Marcinkowska, M.; Śniecikowska, J.; Więckowski, K.; Pawłowski, M.; Głuch-Lutwin, M.; Gryboś, A.; Siwek, A.; Pytka, K.; Jastrzębska-Więsek, M.; Partyka, A.; Wesołowska, A.; Mierzejewski, P.; Kołaczkowski, M. Novel 3-(1,2,3,6-Tetrahydropyridin-4-Yl)-1H-Indole-Based Multifunctional Ligands with Antipsychotic-Like, Mood-Modulating, and Procognitive Activity. *J. Med. Chem.* **2017**, *60* (17), 7483–7501.

(39) Nygaard, R.; Frimurer, T. M.; Holst, B.; Rosenkilde, M. M.; Schwartz, T. W. Ligand Binding and Micro-Switches in 7TM Receptor Structures. *Trends Pharmacol. Sci.* **2009**, *30* (5), 249–259.

(40) Vacher, B.; Maurel, J. L.; Brunel, S. Method for Preparing (3-Chloro-4-Fluorophenyl)-(4-Fluoro-4-{[(5methyl-Pyrimidin-2-Ylmethyl)-Amino]-Methyl}-Piperidin-1-Yl)-Methanone and Novel Intermediate Pyrimidine Derivatives. WO2007039499A1, September 22, 2006.

(41) Maurel, J. L.; Bonnaud, B.; Ribet, J.-P.; Vacher, B. Synthesis Method and Intermediates of Pyridin-2-Yl-Methylamine. WO2002064585A1, February 11, 2002.

(42) Jończyk, A.; Fedoryński, M.; Mąkosza, M. Reactions of Organic Anions. XLIII. Catalytic Method for Synthesis of Glycidic Nitriles in Aqueous Medium. *Tetrahedron Lett.* **1972**, *13* (23), 2395–2396.

(43) Vacher, B.; Bonnaud, B.; Funes, P.; Jubault, N.; Koek, W.; Assié, M.-B.; Cosi, C.; Kleven, M. Novel Derivatives of 2-Pyridinemethylamine as Selective, Potent, and Orally Active Agonists at 5-HT1A Receptors. *J. Med. Chem.* **1999**, *42* (9), 1648–1660.

(44) Suga, H.; Hamatani, T.; Schlosser, M. Regioselective Formation of Fluorohydrins and Their Stereoselective Conversion to Fluoroolefins. *Tetrahedron* **1990**, *46* (12), 4247–4254.

(45) Lipinski, C. A.; Lombardo, F.; Dominy, B. W.; Feeney, P. J. Experimental and Computational Approaches to Estimate Solubility and Permeability in Drug Discovery and Development Settings. *Adv. Drug Deliv. Rev.* **2001**, *46* (1–3), 3–26.

(46) Wager, T. T.; Hou, X.; Verhoest, P. R.; Villalobos, A. Moving beyond Rules: The Development of a Central Nervous System Multiparameter Optimization (CNS MPO) Approach To Enable Alignment of Druglike Properties. *ACS Chem. Neurosci.* **2010**, *1* (6), 435–449.

(47) Waring, M. J.; Arrowsmith, J.; Leach, A. R.; Leeson, P. D.; Mandrell, S.; Owen, R. M.; Pairaudeau, G.; Pennie, W. D.; Pickett, S. D.; Wang, J.; Wallace, O.; Weir, A. An Analysis of the Attrition of Drug Candidates from Four Major Pharmaceutical Companies. *Nat. Rev. Drug Discov.* **2015**, *14* (7), 475–486.

(48) Wager, T. T.; Chandrasekaran, R. Y.; Hou, X.; Troutman, M. D.; Verhoest, P. R.; Villalobos, A.; Will, Y. Defining Desirable Central Nervous System Drug Space through the Alignment of Molecular Properties, in Vitro ADME, and Safety Attributes. *ACS Chem. Neurosci.* **2010**, *1* (6), 420–434.

(49) Tarcsay, A.; Nyíri, K.; Keseru, G. M. Impact of Lipophilic Efficiency on Compound Quality. *J. Med. Chem.* **2012**, *55* (3), 1252–1260.

(50) Dahlin, J. L.; Nissink, J. W. M.; Strasser, J. M.; Francis, S.; Higgins, L.; Zhou, H.; Zhang, Z.; Walters, M. A. PAINS in the Assay: Chemical Mechanisms of Assay Interference and Promiscuous Enzymatic Inhibition Observed during a Sulfhydryl-Scavenging HTS. *J. Med. Chem.* **2015**, *58* (5), 2091–2113.

(51) Pouliot, M.; Jeanmart, S. Pan Assay Interference Compounds (PAINS) and Other Promiscuous Compounds in Antifungal Research. *J. Med. Chem.* **2016**, *59* (2), 497–503.

(52) Brenk, R.; Schipani, A.; James, D.; Krasowski, A.; Gilbert, I. H.; Frearson, J.; Wyatt, P. G. Lessons Learnt from Assembling Screening Libraries for Drug Discovery for Neglected Diseases. *Chemmedchem* **2008**, *3* (3), 435–444.

(53) Daina, A.; Michielin, O.; Zoete, V. SwissADME: A Free Web Tool to Evaluate Pharmacokinetics, Drug-Likeness and Medicinal Chemistry Friendliness of Small Molecules. *Sci. Rep.* **2017**, *7*, 42717.

(54) Bowes, J.; Brown, A. J.; Hamon, J.; Jarolimek, W.; Sridhar, A.; Waldron, G.; Whitebread, S. Reducing Safety-Related Drug Attrition: The Use of in Vitro Pharmacological Profiling. *Nat. Rev. Drug Discov.* **2012**, *11* (12), 909–922.

(55) Gintant, G.; Sager, P. T.; Stockbridge, N. Evolution of Strategies to Improve Preclinical Cardiac Safety Testing. *Nat. Rev. Drug Discov.* **2016**, *15* (7), 457–471. https://doi.org/10.1038/nrd.2015.34.

(56) Di, L.; Kerns, E. H. *Drug-like Properties: Concepts, Structure Design and Methods: From ADME to Toxicity Optimization*; Academic Press: Burlington, MA, 2010.

(57) Wood, C.; Williams, C.; Waldron, G. J. Patch Clamping by Numbers. *Drug Discov. Today* **2004**, *9* (10), 434–441.

(58) Research, C. for D. E. and. About the Center for Drug Evaluation and Research - The Biopharmaceutics Classification System (BCS) Guidance https://www.fda.gov/aboutfda/centersoffices/officeofmedicalproductsandtobacco/cder/ucm128219.htm (accessed Feb 14, 2018).

(59) Doi, S.; Mori, T.; Uzawa, N.; Arima, T.; Takahashi, T.; Uchida, M.; Yawata, A.; Narita, M.; Uezono, Y.; Suzuki, T.; Narita, M. Characterization of Methadone as a β-Arrestin-Biased μ-Opioid Receptor Agonist. *Mol. Pain* **2016**, *12*, 1–9.

(60) Obach, R. S.; Baxter, J. G.; Liston, T. E.; Silber, B. M.; Jones, B. C.; MacIntyre, F.; Rance, D. J.; Wastall, P. The Prediction of Human Pharmacokinetic Parameters from Preclinical and in Vitro Metabolism Data. *J. Pharmacol. Exp. Ther.* **1997**, *283* (1), 46–58.

(61) Banker, M. J.; Clark, T. H.; Williams, J. A. Development and Validation of a 96-Well Equilibrium Dialysis Apparatus for Measuring Plasma Protein Binding. *J. Pharm. Sci.* **2003**, *92* (5), 967–974.

(62) Polli, J. W.; Wring, S. A.; Humphreys, J. E.; Huang, L.; Morgan, J. B.; Webster, L. O.; Serabjit-Singh, C. S. Rational Use of in Vitro P-Glycoprotein Assays in Drug Discovery. *J. Pharmacol. Exp. Ther.* **2001**, *299* (2), 620–628.

(63) Stresser, D. M.; Blanchard, A. P.; Turner, S. D.; Erve, J. C. L.; Dandeneau, A. A.; Miller, V. P.; Crespi, C. L. Substrate-Dependent Modulation of CYP3A4 Catalytic Activity: Analysis of 27 Test Compounds with Four Fluorometric Substrates. *Drug Metab. Dispos.* **2000**, *28* (12), 1440–1448.

(64) Ono, S.; Hatanaka, T.; Hotta, H.; Satoh, T.; Gonzalez, F. J.; Tsutsui, M. Specificity of Substrate and Inhibitor Probes for Cytochrome P450s: Evaluation of in Vitro Metabolism Using CDNA-Expressed Human P450s and Human Liver Microsomes. *Xenobiotica* **1996**, *26* (7), 681–693.

(65) van Wijngaarden, I.; Tulp, M. T.; Soudijn, W. The Concept of Selectivity in 5-HT Receptor Research. *Eur. J. Pharmacol.* **1990**, *188* (6), 301–312.

(66) Hamon, M.; Fattaccini, C. M.; Adrien, J.; Gallissot, M. C.; Martin, P.; Gozlan, H. Alterations of Central Serotonin and Dopamine Turnover in Rats Treated with Ipsapirone and Other 5-Hydroxytryptamine1A Agonists with Potential Anxiolytic Properties. *J. Pharmacol. Exp. Ther.* **1988**, *246* (2), 745–752.

(67) Foreman, M. M.; Fuller, R. W.; Leander, J. D.; Benvenga, M. J.; Wong, D. T.; Nelson, D. L.; Calligaro, D. O.; Swanson, S. P.; Lucot, J. B.; Flaugh, M. E. Preclinical Studies on LY228729: A Potent and Selective Serotonin1A Agonist. *J. Pharmacol. Exp. Ther.* **1993**, *267* (1), 58–71.

(68) Chilmonczyk, Z.; Bojarski, A. J.; Pilc, A.; Sylte, I. Functional Selectivity and Antidepressant Activity of Serotonin 1A Receptor Ligands. *Int. J. Mol. Sci.* **2015**, *16* (8), 18474–18506.

(69) Rojas, P. S.; Fiedler, J. L. What Do We Really Know About 5-HT1A Receptor Signaling in Neuronal Cells? *Front. Cell. Neurosci.* **2016**, *10*, 272.

(70) Stroth, N.; Niso, M.; Colabufo, N. A.; Perrone, R.; Svenningsson, P.; Lacivita, E.; Leopoldo, M. Arylpiperazine Agonists of the Serotonin 5-HT1A Receptor Preferentially Activate CAMP Signaling versus Recruitment of β-Arrestin-2. *Bioorg. Med. Chem.* **2015**, *23* (15), 4824–4830.

(71) Brust, T. F.; Hayes, M. P.; Roman, D. L.; Burris, K. D.; Watts, V. J. Bias Analyses of Preclinical and Clinical D2 Dopamine Ligands: Studies with Immediate and Complex Signaling Pathways. *J. Pharmacol. Exp. Ther.* **2015**, *352* (3), 480–493.

(72) Griffin, M. T.; Figueroa, K. W.; Liller, S.; Ehlert, F. J. Estimation of Agonist Activity at G Protein-Coupled Receptors: Analysis of M2 Muscarinic Receptor Signaling through Gi/o,Gs, and G15. *J. Pharmacol. Exp. Ther.* **2007**, *321* (3), 1193–1207.

(73) Ehlert, F. J. On the Analysis of Ligand-Directed Signaling at G Protein-Coupled Receptors. *Naunyn. Schmiedebergs Arch. Pharmacol.* **2008**, *377* (4–6), 549–577.

(74) Rajagopal, S.; Ahn, S.; Rominger, D. H.; Gowen-MacDonald, W.; Lam, C. M.; Dewire, S. M.; Violin, J. D.; Lefkowitz, R. J. Quantifying Ligand Bias at Seven-Transmembrane Receptors. *Mol. Pharmacol.* **2011**, *80* (3), 367–377.

(75) Fumagalli, F.; Molteni, R.; Calabrese, F.; Frasca, A.; Racagni, G.; Riva, M. A. Chronic Fluoxetine Administration Inhibits Extracellular Signal-Regulated Kinase 1/2 Phosphorylation in Rat Brain. *J. Neurochem.* **2005**, *93* (6), 1551–1560.

(76) Dwivedi, Y.; Zhang, H. Altered ERK1/2 Signaling in the Brain of Learned Helpless Rats: Relevance in Vulnerability to Developing Stress-Induced Depression. *Neural Plast.* **2016**, *2016*, 7383724.

(77) Dwivedi, Y.; Rizavi, H. S.; Roberts, R. C.; Conley, R. C.; Tamminga, C. A.; Pandey, G. N. Reduced Activation and Expression of ERK1/2 MAP Kinase in the Post-Mortem Brain of Depressed Suicide Subjects. *J. Neurochem.* **2001**, *77* (3), 916–928.

(78) Dwivedi, Y.; Rizavi, H. S.; Zhang, H.; Roberts, R. C.; Conley, R. R.; Pandey, G. N. Aberrant Extracellular Signal-Regulated Kinase (ERK)1/2 Signalling in Suicide Brain: Role of ERK Kinase 1 (MEK1). *Int. J. Neuropsychopharmacol.* **2009**, *12* (10), 1337–1354.

(79) First, M.; Gil-Ad, I.; Taler, M.; Tarasenko, I.; Novak, N.; Weizman, A. The Effects of Fluoxetine Treatment in a Chronic Mild Stress Rat Model on Depression-Related Behavior, Brain Neurotrophins and ERK Expression. *J. Mol. Neurosci.* **2011**, *45* (2), 246.

(80) Xiong, Z.; Jiang, B.; Wu, P.-F.; Tian, J.; Shi, L.-L.; Gu, J.; Hu, Z.-L.; Fu, H.; Wang, F.; Chen, J.-G. Antidepressant Effects of a Plant-Derived Flavonoid Baicalein Involving Extracellular Signal-Regulated Kinases Cascade. *Biol. Pharm. Bull.* **2011**, *34* (2), 253–259.

(81) Qi, X.; Lin, W.; Li, J.; Pan, Y.; Wang, W. The Depressive-like Behaviors Are Correlated with Decreased Phosphorylation of Mitogen-Activated Protein Kinases in Rat Brain Following Chronic Forced Swim Stress. *Behav. Brain Res.* **2006**, *175* (2), 233–240.

(82) Qi, X.; Lin, W.; Li, J.; Li, H.; Wang, W.; Wang, D.; Sun, M. Fluoxetine Increases the Activity of the ERK-CREB Signal System and Alleviates the Depressive-like Behavior in Rats Exposed to Chronic Forced Swim Stress. *Neurobiol. Dis.* **2008**, *31* (2), 278–285.

(83) Moyano, S.; Del Río, J.; Frechilla, D. Role of Hippocampal CaMKII in Serotonin 5-HT(1A) Receptor-Mediated Learning Deficit in Rats. *Neuropsychopharmacol. Off. Publ. Am. Coll. Neuropsychopharmacol.* **2004**, *29* (12), 2216–2224.

(84) Buritova, J.; Berrichon, G.; Cathala, C.; Colpaert, F.; Cussac, D. Region-Specific Changes in 5-HT1A Agonist-Induced Extracellular Signal-Regulated Kinases 1/2 Phosphorylation in Rat Brain: A Quantitative ELISA Study. *Neuropharmacology* **2009**, *56* (2), 350–361.

(85) Porsolt, R. D.; Anton, G.; Blavet, N.; Jalfre, M. Behavioural Despair in Rats: A New Model Sensitive to Antidepressant Treatments. *Eur. J. Pharmacol.* **1978**, *47* (4), 379–391.

(86) Yankelevitch-Yahav, R.; Franko, M.; Huly, A.; Doron, R. The Forced Swim Test as a Model of Depressive-like Behavior. *J. Vis. Exp. JoVE* **2015**, No. *97*, e52587.

(87) Assié, M.-B.; Bardin, L.; Auclair, A. L.; Carilla-Durand, E.; Depoortère, R.; Koek, W.; Kleven, M. S.; Colpaert, F.; Vacher, B.; Newman-Tancredi, A. F15599, a Highly Selective Post-Synaptic 5-HT(1A) Receptor Agonist: In-Vivo Profile in Behavioural Models of Antidepressant and Serotonergic Activity. *Int. J. Neuropsychopharmacol.* **2010**, *13* (10), 1285–1298.

(88) Kołaczkowski, M.; Mierzejewski, P.; Bienkowski, P.; Wesołowska, A.; Newman-Tancredi, A. Antipsychotic, Antidepressant, and Cognitive-Impairment Properties of Antipsychotics: Rat Profile and Implications for Behavioral and Psychological Symptoms of Dementia. *Naunyn. Schmiedebergs Arch. Pharmacol.* **2014**, *387* (6), 545–557.

(89) Yang, C.; Hu, Y.-M.; Zhou, Z.-Q.; Zhang, G.-F.; Yang, J.-J. Acute Administration of Ketamine in Rats Increases Hippocampal BDNF and MTOR Levels during Forced Swimming Test. *Ups. J. Med. Sci.* **2013**, *118* (1), 3–8.

(90) Kołaczkowski, M.; Bucki, A.; Feder, M.; Pawłowski, M. Ligand-Optimized Homology Models of D1 and D2 Dopamine Receptors: Application for Virtual Screening. *J. Chem. Inf. Model.* **2013**, *53* (3), 638–648.

(91) Wang, C.; Jiang, Y.; Ma, J.; Wu, H.; Wacker, D.; Katritch, V.; Han, G. W.; Liu, W.; Huang, X.-P.; Vardy, E.; McCorvy, J. D.; Gao, X.; Zhou, X. E.; Melcher, K.; Zhang, C.; Bai, F.; Yang, H.; Yang, L.; Jiang, H.; Roth, B. L.; Cherezov, V.; Stevens, R. C.; Xu, H. E. Structural Basis for Molecular Recognition at Serotonin Receptors. *Science* **2013**, *340* (6132), 610–614.

(92) Kurowski, M. A.; Bujnicki, J. M. GeneSilico Protein Structure Prediction Meta-Server. *Nucleic Acids Res.* **2003**, *31* (13), 3305–3307.

(93) Schwede, T.; Kopp, J.; Guex, N.; Peitsch, M. C. SWISS-MODEL: An Automated Protein Homology-Modeling Server. *Nucleic Acids Res.* **2003**, *31* (13), 3381–3385.

(94) Sherman, W.; Day, T.; Jacobson, M. P.; Friesner, R. A.; Farid, R. Novel Procedure for Modeling Ligand/Receptor Induced Fit Effects. *J. Med. Chem.* **2006**, *49* (2), 534–553.

(95) Hidalgo, I. J.; Raub, T. J.; Borchardt, R. T. Characterization of the Human Colon Carcinoma Cell Line (Caco-2) as a Model System for Intestinal Epithelial Permeability. *Gastroenterology* **1989**, *96* (3), 736–749.

(96) Mathes, C. QPatch: The Past, Present and Future of Automated Patch Clamp. *Expert Opin. Ther. Targets* **2006**, *10* (2), 319–327.

(97) Pauwels, P. J.; Colpaert, F. C. Ca2+ Responses in Chinese Hamster Ovary-K1 Cells Demonstrate an Atypical Pattern of Ligand-Induced 5-HT1A Receptor Activation. *J. Pharmacol. Exp. Ther.* **2003**, *307* (2), 608–614.

(98) Detke, M. J.; Rickels, M.; Lucki, I. Active Behaviors in the Rat Forced Swimming Test Differentially Produced by Serotonergic and Noradrenergic Antidepressants. *Psychopharmacology (Berl.)* **1995**, *121* (1), 66–72.

(99) Kleven, M. S.; Assié, M. B.; Koek, W. Pharmacological Characterization of in Vivo Properties of Putative Mixed 5-HT1A Agonist/5-HT(2A/2C) Antagonist Anxiolytics. II. Drug Discrimination and Behavioral Observation Studies in Rats. *J. Pharmacol. Exp. Ther.* **1997**, *282* (2), 747–759.

(100) Draft Guidance for Industry on Bioanalytical Method Validation; Availability https://www.federalregister.gov/documents/2013/09/13/2013-22309/draft-guidance-for-industry-on-bioanalytical-method-validation-availability (accessed Mar 1, 2018).

TABLE OF CONTENTS GRAPHIC